WAVELET TRANSFORMS

Functions that oscillate over time are often called waves. If the function is such that it oscillates only in a localized region and goes to zero outside the region it may be called a wavelet. Thus we say wavelets are localized waves. This is analogous to many processes in nature. Consider a sound wave that starts out at zero, builds to some maximum, and then dies out to zero. If the duration of the sound is a few seconds we say the scale for the process is on the order of seconds. Whenever examining some physical object scale plays an important role. For example, when looking at another human at a scale of about a meter you see the whole individual, but if you examine the same individual at a scale of about a centimeter you can see details such as whorled ridges that form the fingerprint.

The fundamental role of the wavelet transform is to facilitate the analysis of signals or images according to scale. Wavelets are functions with some very special mathematical properties that serve as a tool for efficiently dividing data into a sequence of frequency components without losing all information about position. This can be thought of in terms of viewing an object through different size windows. If a large window is used we see gross features, and if a small window is used we only see small detail features. There are many similarities between wavelet analysis and classical windowed Fourier analysis. The goal in the latter is to determine the local frequency content of a signal by using sine and cosine functions multiplied by a sliding window. The wavelet analysis makes use of translations and dilations of an oscillating wavelet, called the *mother wavelet,* to characterize both spatial and frequency contents of a signal. The properties of this analyzing wavelet are very different from those of sines and cosines. These differences make it possible to approximate a signal contained in a finite region or a signal with sharp changes with a few coefficients, something not possible with classical Fourier methods.

Many of the principles that are the foundation for wavelet analysis emerged independently in mathematics, physics, geophysics, and engineering. In most cases the concepts came from the motivation to solve some problem that related to resolution or scale. During the last decade wavelets have been used with great success in a very wide variety of areas, including image compression, coding, signal processing, numerical analysis, turbulence, acoustics, seismology, and medical imaging.

There are some basic mathematical concepts that must be understood prior to a full explanation of the two types of wavelet transforms, the continuous transform and the discrete transform. The next section on basic concepts from linear algebra and Fourier analysis can be skipped by those who have already reached that level of mathematical sophistication.

BASIC CONCEPTS

Basis

One of the most fundamental ideas associated with many areas of mathematics is the concept of a *basis.* A simple illustration serves to get the idea across. Suppose we have a curve (waveform or signal) that looks somewhat complicated, as in Fig. 1. (In practice this could be a voltage that varies in time.) How could you explain to someone who could not see the curve just what it looks like? One possible way is to think of the complicated curve as being made up of the sum of several simple curves. The complicated curve is selected so that it is exactly the sum of two simple curves shown in Fig. 2. The simple curves are known as sine curves. These fundamental curves can be described in terms of how many times they go through a complete cycle. Note that the low-frequency curve goes through one cycle and the higher frequency curve goes through three cycles. Also note that the low-frequency curve has two times the amplitude of the high frequency curve. You could tell someone exactly how to reproduce the more complicated curve by giving the information about frequency and amplitude for the two basic curves. For those familiar with formulas for sine curves, the complicated curve is given by $y = 2 \sin(2\pi x) + \sin(6\pi x)$.

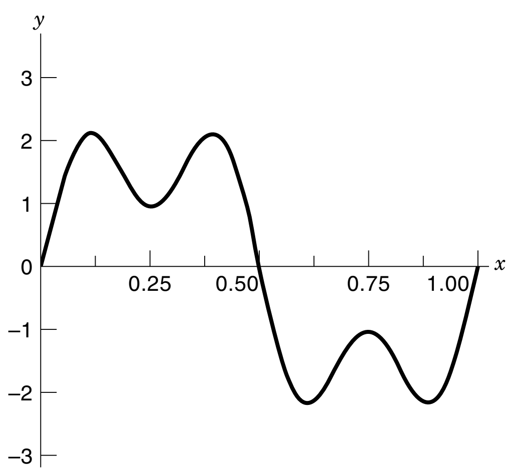

Figure 1. A complicated curve.

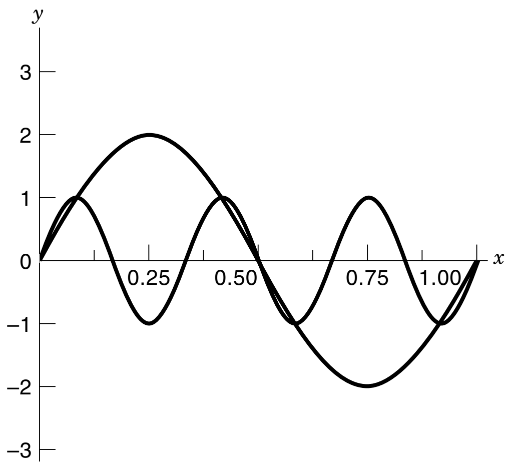

Figure 2. Two simple curves. The curve in Fig. 1 is the sum of these two curves.

Technical Definitions: Motion that repeats in equal intervals of time is called periodic. The *period* is the time required for one complete cycle or oscillation. The *frequency* is the repetition rate of a periodic process. This is the number of cycles that occur over a given interval of time. If the period is given in seconds, the frequency is in hertz, abbreviated Hz. In Fig. 2, if the x axis represents time (in seconds) the frequencies are 1 Hz and 3 Hz for the two curves.

The concept of a basis comes from an extension of the approach used to produce the curve in Fig. 1 from the sum of the curves in Fig. 2. If the basis is selected so that it is complete, an arbitrary curve can be replaced by a sum of basic curves. When this is done for periodic functions using sine or cosine curves with different frequencies and amplitudes it is called a Fourier series decomposition. If the original function is not periodic and can be defined over the entire x axis such that its area is finite, a Fourier transform is used.

The important concept here is that there is a formal way to represent a function or waveform as a sum of basic parts. Fourier analysis corresponds to the language used, and there is a prescription for calculating the coefficients in the sum. This corresponds to finding the amplitudes in Fig. 2. You might think of this as a sort of mathematical prism. The prism breaks light into various colors in much the same way the Fourier analysis breaks the complicated waveform into component parts.

When considering all sorts of waveforms an obvious question emerges. Under just what conditions is Fourier analysis the appropriate mathematical language to use to decompose the waveform? The complete answer to this question is the subject of the enormous literature on Fourier series and Fourier transforms. There are some simple answers that will suffice for our purposes. The sum in a typical Fourier series problem is an infinite sum. This means an infinite number of coefficients must be computed to represent the function. It seems we have made the problem more complicated! It turns out that in many physical situations only a few coefficients are needed to give an adequate description of the waveform. The coefficients associated with the high-frequency sines and cosines approach zero as the frequency increases. You can think about it this way: The large coefficients correspond to the case where there is a fair match between the original function and the basic sine or cosine. If the original waveform changes slowly relative to the high-frequency oscillations there is a poor match, and consequently the coefficients are very small. More will be said about this in the sections that follow.

Orthogonality

Another concept that is essential is that of *orthogonality.* Recall from elementary geometry, if two line segments are perpendicular we say they are orthogonal. If we make vectors out of line segments by giving them properties of magnitude and direction we can determine whether they are orthogonal or not by computing their *scalar* product. This is sometimes called the *dot* or *inner* product. If the scalar product is zero they are orthogonal. Another way to think about this is that orthogonal vectors do not have any components in common, or they contain completely independent information. The same type of thing can be defined for functions; however, the rule for doing the scalar product is different. It involves doing an integral of the product of two functions. The coefficients in a Fourier series expansion can be found by computing scalar products of the original waveform multiplied by sine and cosine functions with different frequencies. The important point is that the building blocks, the sines and cosines of different frequencies, are orthogonal and complete. An important consequence is that the frequency content of the waveform can be determined in an unambiguous way. Also, an orthogonal transformation allows perfect reconstruction of the original waveform and eliminates redundancy. Generally, orthogonal transformations are more efficient and easier to use.

Sampling and the Fast Fourier Transform

In nature many waveforms are continuous functions of time. If we want to work with these signals using digital computers it is necessary to find a discrete representation. This means we have to *sample* the continuous function. There is an extremely important theorem known as the *Shannon sampling theorem* that is invoked in these situations. Proofs are given in most standard texts on Fourier analysis, for example, Bracewell (1) and Brigham (2). The theorem states that a continuous signal can be represented completely by and reconstructed perfectly from a set of measurements (samples) of its amplitude made at equally spaced times. The time interval between samples must be equal to or less than one-half the period of the highest frequency present in the signal. For example, for a typical voice signal the frequency range is from 0 Hz to 4,000 Hz. This signal must be sampled 8,000 times per second in order to describe it perfectly. In practice the idea of perfect reconstruction must be compromised. When the amplitude is sampled with real physical apparatus there must be some sort of round off. In speech transmission an error of 1% is often sufficient for practical purposes.

Another development that helped usher in the digital communication revolution is the *Fast Fourier Transform* (FFT). For n sampled points this reduces the number of computations from n^2 to $n \log n$. This is especially important for large values of n. A very interesting discussion of the FFT is given by Heideman, Johnson, and Burrus (3).

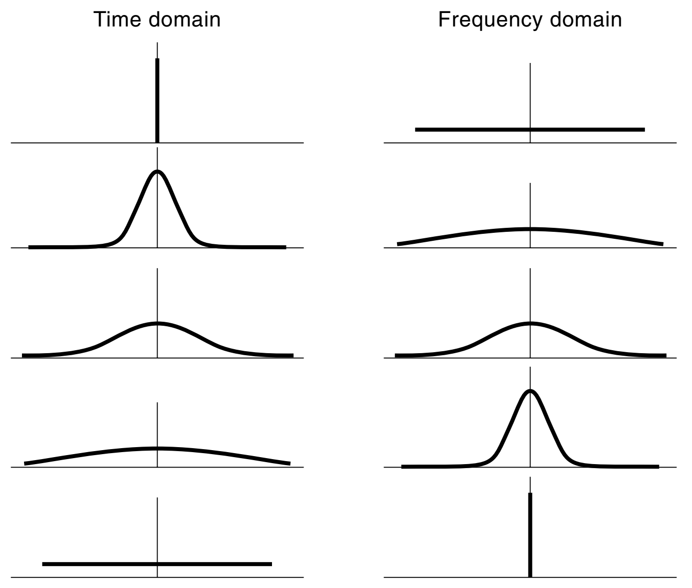

Figure 3. Signals concentrated in one domain are spread in the other domain.

Time and Frequency Domains

When we look at the signal in the time domain we have full information about the amplitude of the signal at any time. When we do the Fourier decomposition we have full information about the frequency content of the signal, but the time information is not apparent. The inverse transform yields the time information, but then the frequency spectrum is not apparent. Another way to think about this is to observe that a very sharp signal in the time domain is flat in the frequency domain. Inspection of the frequency spectrum does not tell when the sharp signal occurred in time. Some time domain and frequency domain transform pairs are shown in Fig. 3. The important point is that signals localized in time are spread in frequency and those spread in time are localized in frequency.

CLASSIFICATION OF SIGNALS

It is useful to give a broad classification of signals as *stationary, quasi-stationary,* and *nonstationary.* A signal is *stationary* if its statistical properties are invariant over the time duration of the signal. For these signals the probability of unexpected events is known in advance. If there are transient events (such as blips or discontinuities) in the signal that cannot be predicted, even with knowledge of the past, the signal is *nonstationary.* Consider viewing the signal through a window of some width; that is, look at a section of the signal. A signal is called *quasi-stationary* if the signal is stationary at the scale of the window.

The ideal tool for studying stationary signals is Fourier analysis. The study of nonstationary signals requires other techniques. One of these is the use of wavelets. An important technique for the study of quasi-stationary signals came before wavelets and will be discussed first.

The desire to maintain information about time when doing Fourier decompositions leads to the short-time Fourier transform (STFT), sometimes called the windowed Fourier trans-

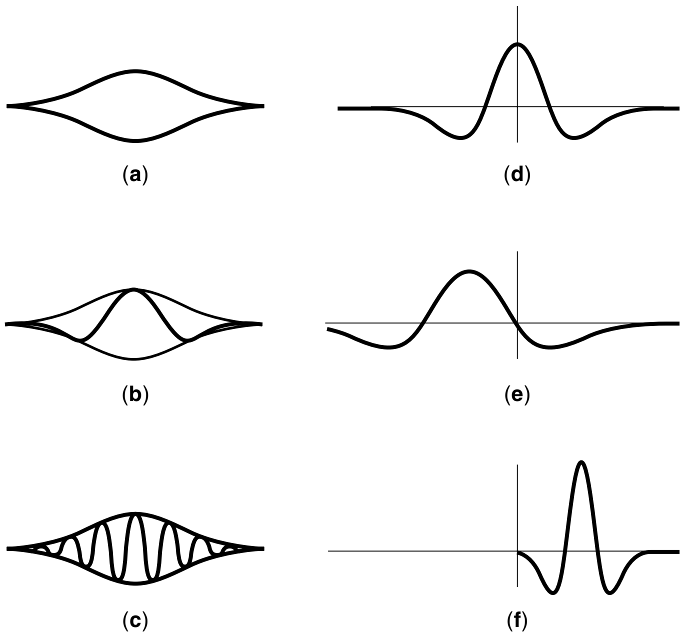

Figure 4. Comparison of STFT and wavelets. On the left, select the window and allow different frequency sinusoids to fill the window. On the right, select the mother wavelet, then translate and dilate the wavelet. The second wavelet is expanded and shifted to the left. The third wavelet is compressed and shifted to the right.

form. The idea is to select a window with fixed width and slide it along the signal. The Fourier decomposition is done for several short times of the signal rather than for the entire signal all at once. By a proper choice of the window it is possible to maintain both time and frequency information; thus, this transformation is known as a time–frequency decomposition. When the window is a Gaussian the transform is known as a Gabor transform in honor of early work done by Dennis Gabor (4). Difficulties in connection with this approach involve both orthogonality and invertibility. An introduction to the STFT and the wavelet transform is given by Rioul and Vetterli (5). The close connection with wavelets is illustrated in Fig. 4. Note that the main difference is that the functional form of the wavelet does not change, hence the name *mother wavelet.* The choices for the mother wavelet are virtually unlimited. This is in sharp contrast to Fourier analysis where the basis functions are sines and cosines.

The mother wavelet is allowed to undergo translations and dilations. It is the various translations and dilations of the mother wavelet that form the basis functions for the wavelet transform. This stretching or compressing of the wavelet changes the size of the window and allows the analysis of signals at different scales. This is in some sense like a microscope; the wide stretched out wavelets are used to give a broad approximate image of the signal while the smaller and smaller compressed wavelets can zoom in on finer and finer details.

TIME–FREQUENCY RESOLUTION

We have already seen that sharp signals in the time domain correspond to flatness in the frequency domain. If the window for the STFT is selected as in the third row of Fig. 3 then the tiles that represent the essential concentration in the time–frequency plane are squares as indicated on the left in Fig. 5. For a window fixed at one position along the time axis, going up vertically corresponds to higher and higher frequency sinusoidal curves contained within the window. The corresponding tiles for the wavelet transform are shown on the right in Fig. 5. Here the wavelet that is stretched out over the time axis (low frequency) has a narrow concentration in the frequency domain. As the wavelet is compressed (higher fre-

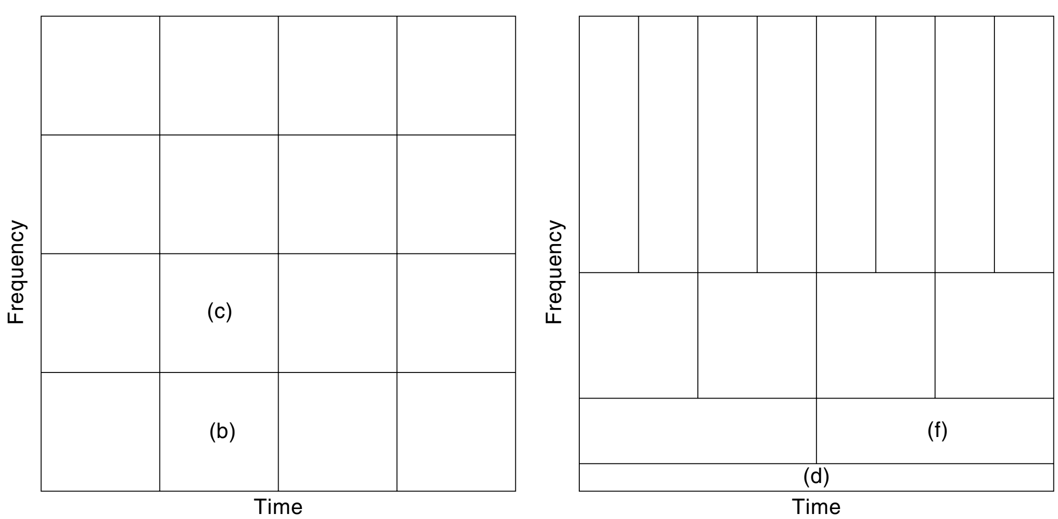

Figure 5. Left: Time and frequency resolution for STFT. Right: Time and frequency resolution for WT. The tiles indicate the region of concentration in the time–frequency plane for a basis function. As an illustration, if the tile labeled (b) corresponds to (b) in Fig. 4, then tile (c) could correspond to (c) in Fig. 4. The corresponding comparison for wavelets is for tiles labeled (d) and (f) with (d) and (f) in Fig. 4.

quencies, smaller time window) the concentration in the frequency domain is less and less concentrated. Think about this in terms of the curves in Fig. 3 where small time windows correspond to broad frequency windows. This helps in understanding how scale plays such an important role in the wavelet transform.

SOME HISTORY

There are many avenues that can be followed in trying to trace the history of wavelets. Barbara Burke Hubbard (6) has a quote in her beautiful discussion of wavelets by Yves Meyer. He says: “I have found at least 15 distinct roots of the theory, some going back to the 1930s.” Seven of these sources in pure mathematics are discussed in some detail in the translation of some Meyer’s (7) lecture notes. The reader with some background in harmonic analysis will find this discussion covering 70 years of mathematics fascinating: the Haar basis (1909), the Franklin orthonormal system (1927), Littlewood–Paley theory (1930), Calderón–Zygmund theory (1960–1978), and the work of Strömberg (1980). In addition to the lecture notes by Meyer, references for this background include Haar (8), Franklin (9), Hernández and Weiss (10), Edwards and Gaudry (11) for Littlewood–Paley theory, Stein (12) for Calderón–Zygmund theory, and Strömberg (13).

This work done by mathematicians is now understood as part of the history of wavelets. The term “atomic decompositions” was used in place of the term wavelets. During this period from 1910 to 1980, mathematicians from the University of Chicago (location of Zygmund and Calderón) were leaders in harmonic analysis, but apparently they did not interact very much with the experts in physics and signal processing.

In physics, the ideas underlying wavelets are present in Nobel laureate Kenneth Wilson’s (14) work on the renormalization group. A review of some of Wilson’s work and other uses of wavelets in physics is given by Guy Battle (15,16). Wavelet concepts also appear in the study of coherent states in quantum mechanics. This work dates from the early 1960s by Glauber (17) and Aslaksen and Klauder (18,19).

In parallel with advances in mathematics and physics there were important ideas fundamental to wavelets being developed in signal and image processing. This work was mostly in the context of discrete-time signals. As is often the case in applied science much of this work was driven by the need to solve a problem. We have already mentioned the work by Gabor who introduced concepts very close to wavelets in speech and signal processing. A technique called subband coding was proposed by Croisier, Esteban, and Galand (20) for speech and image compression. This work and related work by Esteban and Galand (21) and Crochiere, Webber, and Flanagan (22) made use of special filters known as quadrature mirror filters (QMF). This led to important work in perfect reconstruction filter banks discussed in detail by Vetterli and Kovačević (23). Other important relevant work was the development of pyramidal algorithms in image processing by Burt and Adelson (24), where images are approximated proceeding from a coarse to fine resolution. This idea is similar to the multiresolution framework currently used in connection with the discrete wavelet transform.

The important point of all of this is that the foundations of wavelet transforms were implicit in several areas of science, but those working in the various areas were not communicating outside their own field. The grand unification came as a surprise to many and is certainly one reason why this subject has become so popular. Several people made important contributions to this unification. Yves Meyer, in the foreword to the book by Hernández and Weiss (10), gives special tribute to Alex Grossmann and Stéphane Mallat.

In the early 1980s Jean Morlet, a geophysicist with the French oil company Elf-Aquitaine, coined the name wavelet in connection with analysis of data in oil prospecting [see Morlet et al. (25)]. Morlet’s early work was based on extensions of the Gabor transform coupled with the fundamental idea of holding the number of oscillations in the window constant while varying the width of the window. Morlet developed empirical methods for decomposing a signal into wavelets and then reconstructing the original signal, but it was not clear how general the numerical techniques were. Morlet was referred to Alex Grossmann who had extensive experience in Fourier analysis as utilized in quantum mechanics. it took them about two years to determine that the inversion was exact, and not an approximation [Grossmann and Morlet (26)].

During 1985–1986 Stéphane Mallat (27,28), an expert in computer vision, signal processing, and applied mathematics, discovered some important connections among: (1) the quadrature mirror filters, (2) the pyramid algorithms, and (3) the orthonormal wavelet bases of Strömberg Meyer, building on the work by Mallat, constructed wavelets that are continuously differentiable but they do not have compact support. (A function with compact support vanishes outside a finite interval.) A full discussion of these Meyer wavelets is given by Ingrid Daubechies (29), where she points out that Meyer actually found this basis while trying to prove the nonexistence of such nice wavelet bases. It requires a considerable amount of work to calculate the wavelet coefficients for the Meyer wavelets, and Daubechies wanted to construct wavelets that would be easier to use. She had worked with Grossmann in France on her Ph.D. research in physics and she knew about Mallat and Meyer’s work before it was published. She demanded orthogonality, compact support, and some degree of smoothness (wavelets with vanishing moments). These constraints are so much in conflict that most people doubted such a task could be accomplished. After some very intense work she had the construction by the end of March 1987. See the revealing quote on page 47 of Hubbard (6). This work is elegant and the Daubechies wavelets have become the cornerstone of wavelet applications throughout the world. The first publication on her construction is in Ref. 30. Other relevant descriptions are in Refs. 29 and 31.

This concludes an all too brief history of a topic that has roots reaching into the core of pure and applied mathematics, physics, geophysics, computer science, and engineering. The reader with interest in these matters will find the informal discussion by Ingrid Daubechies (32) both enjoyable and enlightening. In that discussion she does not cite specific references, but all of the characters in the story are identified in the bibliography or reading list for this article or in the books by Vetterli and Kovačević (23) and Daubechies (29).

THE CONTINUOUS WAVELET TRANSFORM

Families of continuous wavelets are found by shifting and scaling a "mother" wavelet $\psi(x)$

$$\psi_{a,b} = \frac{1}{\sqrt{a}}\,\psi\left(\frac{x-b}{a}\right), \qquad a, b \in \mathbb{R}, \quad a \neq 0 \tag{1}$$

The parameter a is the scale parameter, b is the shift parameter, and $\mathbb{R}$ is the set of real numbers. One possible identification for ψ is the Mexican hat function,

$$\psi(x) = \frac{2}{\sqrt{3}}\,\pi^{-1/4}(1-x^2)e^{-1/2x^2}$$

This function is the second derivative of a Gaussian $e^{-1/2x^2}$. The normalization is such that its square integrated over the real line is unity, $L^2(\mathbb{R})$ norm equal to 1. This is the function used for illustration on the right side of Fig. 4. The reason for the name comes from the image generated by a rotation around its axis of symmetry (29). Observe that for large a the basis function $\psi_{a,b}$ is a stretched out version of ψ and small a gives a contracted version.

If the basis functions are required to satisfy a completeness condition, then it is necessary for the wavelet to satisfy an "admissibility" condition (23)

$$C_\psi = \int_{-\infty}^{\infty} \frac{|\hat{\psi}(\xi)|^2}{\xi}\,d\xi < \infty$$

where $\hat{\psi}$ is the Fourier transform of ψ,

$$\hat{\psi}(\xi) = \int_{-\infty}^{\infty} \psi(x)e^{-ix\xi}\,dx$$

This means that for practical cases we must require (Let $\xi \to 0$ in the formula for the Fourier transform):

$$\int_{-\infty}^{\infty} \psi(x)\,dx = \hat{\psi}(0) = 0$$

Thus, the wavelet function cannot be a symmetric positive "bump" function like a Gaussian, but must wiggle around the x axis like a wave. The zero of the Fourier transform at the origin and the decay of the spectrum $\hat{\psi}$ at high frequencies implies that the wavelet has a bandpass behavior.

The continuous wavelet transform of a function $f(x)$ is defined by

$$\tilde{f}(a,b) = \langle \psi_{a,b}, f\rangle = \int_{-\infty}^{\infty} \psi_{a,b}(x)f(x)\,dx \tag{2}$$

for a *real* set of basis functions. The function f is recovered from the transformed function $\tilde{f}$ by the inversion formula

$$f(x) = \frac{1}{C_\psi}\int_{-\infty}^{\infty}\int_{-\infty}^{\infty} \frac{da\,db}{a^2}\tilde{f}(a,b)\psi_{a,b}(x) \tag{3}$$

For a proof, see Chapter 5 of Ref. 23. This last formula says that $f(x)$ can be written as a superposition of shifted and dilated wavelets.

The continuous wavelet transform has an energy conservation property that is similar to Parseval's formula for the Fourier transform. The function $f(x)$ and its continuous wavelet transform $\tilde{f}(a, b)$ satisfy

$$\int_{-\infty}^{\infty} |f(x)|^2\,dx = \frac{1}{C_\psi}\int_{-\infty}^{\infty}\int_{-\infty}^{\infty} \frac{da\,db}{a^2}|\tilde{f}(a,b)|^2 \tag{4}$$

The wavelet transform has localization properties. There is a sharp time localization at high frequencies, in marked contrast with Fourier transforms. For example, the wavelet transform of a delta function centered at x_0 is

$$\frac{1}{\sqrt{a}}\int_{-\infty}^{\infty} \psi\left(\frac{x-b}{a}\right)\delta(x-x_0)\,dx = \frac{1}{\sqrt{a}}\,\psi\left(\frac{x_0-b}{a}\right)$$

For a given scale factor a the transform is equal to a scaled and normalized wavelet centered at the location of the delta function.

DISCRETE WAVELET TRANSFORM

The wavelet transform has to be discretized for most applications. One way to approach this is to attempt to directly discretize the continuous wavelet transform and find a discrete version of the reconstruction formula given in Eq. (3). In effect this means replace $\psi_{a,b}$ by $\psi_{m,n}$ with $m, n \in \mathbb{Z}$, where $\mathbb{Z}$ is the set of integers. The appropriate replacements for a and b are (23,29)

$$a = a_0^m, \quad b = nb_0a_0^m, \quad a_0 > 1, \quad b_0 > 0$$

When this is done, it turns out that in the discrete parameter case there is no direct generalization of Eq. (3); however, for certain ψ and appropriate a_0 and b_0 there exist $\tilde{\psi}_{m,n}$ such that

$$f = \sum_{m,n}\langle \psi_{m,n}, f\rangle \tilde{\psi}_{m,n}$$

This leads to the introduction of *frames* and *dual frames.* These represent an alternative to orthonormal bases in a Hilbert space [see Heil and Walnut (33)]. This approach will not be pursued here. We refer the reader to standard references (10,23,29,33).

The approach presented here leads to the construction of orthonormal wavelet expansions for discrete sets of data. We *do not* start with a continuous wavelet and attempt to find a discrete counterpart. We make full use of multiresolution, the idea of looking at something at various scales or resolutions.

Multiresolution Analysis

In this approach another function ϕ plays a fundamental role along with the wavelet function ψ. The simplest possible system that illustrates most of the fundamental properties of these functions is the Haar scaling function and Haar wavelet. In this case the scaling function is the box function illus-

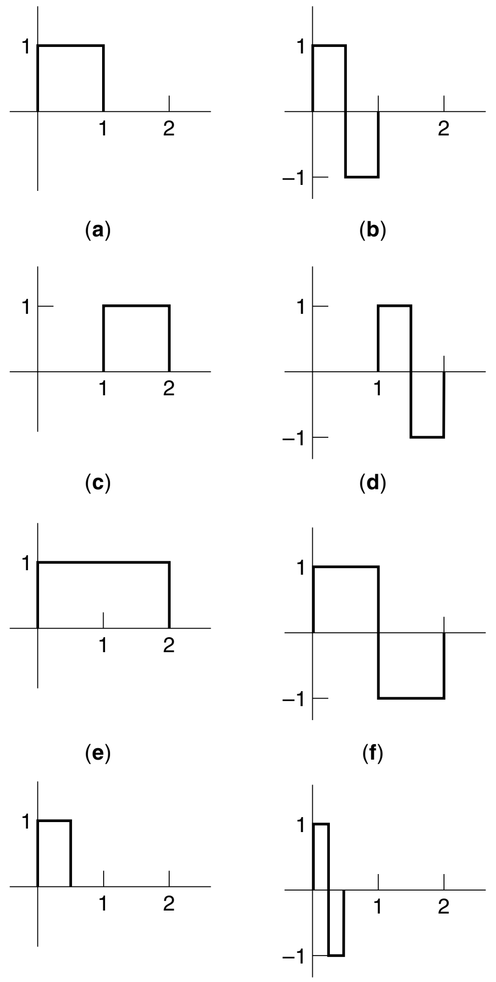

Figure 6. Scaling function ϕ and wavelet function ψ for the Haar system: (a) $\phi(x)$, (b) $\psi(x)$, level 0, basic; (c) $\phi(x - 1)$, (d) $\psi(x - 1)$, level 0, translated; (e) $\phi(\frac{1}{2}x)$, (f) $\psi(\frac{1}{2}x)$, level 1, basic; and (g) $\phi(2x)$, (h) $\psi(2x)$, level -1, basic.

trated in Fig. 6(a) and the corresponding wavelet is shown in Fig. 6(b). We refer to these two functions as the *level 0* functions. The fundamental idea is to construct other scaling functions and wavelets from dilations and translations of the level 0 functions. Some of these are shown in Fig. 6. Note that scaling by $x \to 2x$ corresponds to a contraction and scaling by $x \to \frac{1}{2}x$ gives an expansion. There are two scaling functions and two wavelet functions at level -1, with support on an interval of length $\frac{1}{2}$,

$$\phi(2x), \quad \phi(2x-1), \quad \psi(2x), \quad \psi(2x-1)$$

Complete families of scaling functions and the wavelets are obtained by appropriate translations and dilations. The functions $\phi(x)$ and $\psi(x)$ are the functions at level 0. The move from $\psi(x)$ to $\psi(2x)$ is a dilation operation, whereas the shift from 0 to 1 is a translation operation. Starting from ϕ and ψ the functions are shifted and compressed. The next level down (level -2) contains

$$\phi(4x), \quad \phi(4x-1), \quad \phi(4x-2), \quad \phi(4x-3); \quad \psi(4x), \quad \psi(4x-1), \quad \psi(4x-2), \quad \psi(4x-3)$$

Each of these functions is supported on an interval of length $\frac{1}{4}$. A continuation of this process gives infinite families of functions,

$$\phi_{j,k}(x) = 2^{-j/2}\phi(2^{-j}x-k); \quad \psi_{j,k}(x) = 2^{-j/2}\psi(2^{-j}x-k) \quad (5)$$

with $j, k \in \mathbb{Z}$. For the range of values ($j \le 0$) and ($0 \le k < 2^{-j}$), these functions form a basis over the interval [0, 1].

Important Remark: The Haar system is used for illustration purposes since it is simple and easy to understand. The important point is that all of this holds for other scaling functions and wavelets that have increasing degrees of smoothness. Some of these will be discussed and illustrated later.

Suppose we designate the space spanned by functions of the form $\phi(x - k)$, $k \in \mathbb{Z}$, by V_0 and the space spanned by functions of the form $\phi(2x - k)$, $k \in \mathbb{Z}$, by V_{-1}. Clearly, the function $\phi(x)$ can be written as

$$\phi(x) = \phi(2x) + \phi(2x-1)$$

Since functions in V_0 can be written as a linear combination of functions in V_{-1} we have the condition

$$V_0 \subset V_{-1}$$

This argument can be extended in either direction, for example

$$\phi(\tfrac{1}{2}x) = \phi(x) + \phi(x-1), \quad V_1 \subset V_0$$

An example of the projection of a function onto V_0 and V_1 is shown in Fig. 7. By continuing this process the nesting of the closed subspaces V_j follows,

$$\leftarrow \text{coarser} \ldots V_2 \subset V_1 \subset V_0 \subset V_{-1} \subset V_{-2} \subset \ldots \text{finer} \rightarrow \quad (6)$$

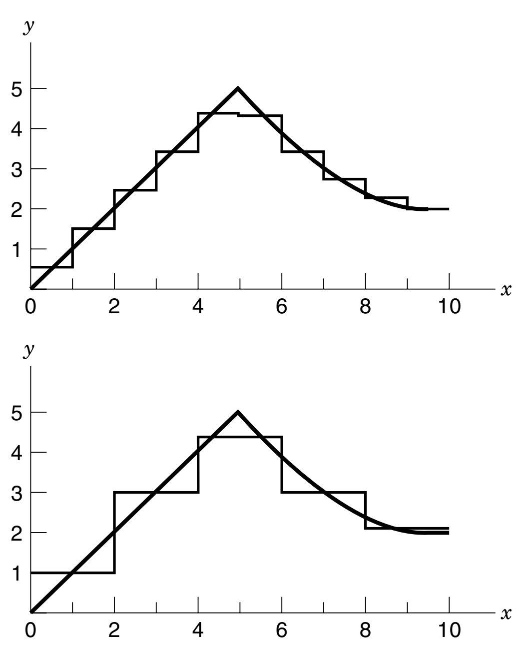

Figure 7. A function $y = f(x)$ (dots) projected onto V_0 (top), projected onto V_1 (bottom).

The nesting order is selected so that the spaces show less detail as the index increases. For example, in Fig. 7 the projection onto V_1 can be considered as a blurred version of the projection onto V_0. This is an agreement with the choice made by Daubechies (29). A caution for the reader is in order on this; about half of the wavelet literature uses the opposite convention, coupled with a change of $-j$ to $+j$ in Eq. (5). Properties of the V_j are summarized by the following definition of an orthogonal multiresolution analysis.

A *multiresolution analysis* of $L^2(\mathbb{R})$ consists of a sequence of closed subspaces V_j, for all $j \in \mathbb{Z}$, such that

(M1) $V_j \subset V_{j-1}$

(M2) $\overline{\bigcup_j V_j} = L^2(\mathbb{R})$ and $\bigcap_j V_j = \{0\}$

(M3) $f(x) \in V_j \Leftrightarrow f(2x) \in V_{j-1}$

(M4) $f(x) \in V_0 \Leftrightarrow f(x-k) \in V_0$ for all $k \in \mathbb{Z}$

(M5) There exists a function $\phi \in V_0$ so that $\phi(x-k), k \in \mathbb{Z}$ form an orthonormal basis for V_0.

Several remarks are in order in regard to this definition. In (M2) the bar over the union is to indicate *closure.* The closure of a set is obtained by including all functions that can be obtained as limits of sequences in the set. This terminology could be replaced by saying that the union is dense in L^2. Condition (M5) is often relaxed by assuming that the set of functions $\phi(x-k)$ is a *Reisz basis* for V_0. For a full treatment of this approach, see Refs. 10 and 34.

Now let us observe that although we have the condition $V_0 \subset V_{-1}$ the basis functions in V_0 are not orthogonal to the basis functions in V_{-1},

$$\int \phi(x)\phi(2x)\,dx \neq 0 \quad \text{and} \quad \int \phi(x)\phi(2x-1)\,dx \neq 0$$

The integrals are over all x where the functions do not vanish. For the Haar case illustrated earlier this would be over the interval [0, 1]. There is a clever way to fix this. Note that we can write

$$\phi(2x) = \tfrac{1}{2}[\phi(x) + \psi(x)] \quad \text{and} \quad \phi(2x-1) = \tfrac{1}{2}[\phi(x) - \psi(x)]$$

If we designate the space spanned by the wavelets $2^{-j/2}\psi(2^{-j}x - k)$, $j, k \in \mathbb{Z}$, by W_j, it follows that the direct sum of subspaces gives

$$V_{-1} = V_0 \oplus W_0$$

Moreover, it is easy to check that basis functions in V_0 are orthogonal to basis functions in W_0. This idea can be extended in either direction

$$V_{-2} = V_{-1} \oplus W_{-1} \quad \text{and} \quad V_0 = V_1 \oplus W_1$$

The space W_j is said to be the *orthogonal complement* of V_j in V_{j-1}. In general we have

$$V_{j-1} = V_j \oplus W_j, \quad W_j \perp W_{j'}, \quad \text{if } j \neq j' \tag{7}$$

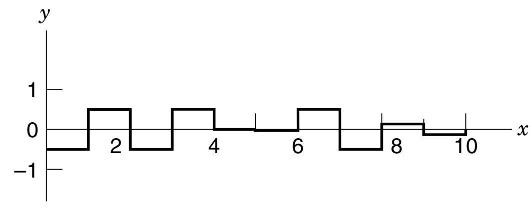

Figure 8. The detail information for the function from Fig. 7 in W_1.

If we designate the projection of $f(x)$ onto V_m by $P_m f$ and the projection of $f(x)$ onto W_m by $Q_m f$, then Eq. (7) implies that

$$P_{j-1}f = P_j f + Q_j f \tag{8}$$

If $j = 1$ this is $P_0 f = P_1 f + Q_1 f$. Projections $P_0 f$ and $P_1 f$ are shown in Fig. 7. The projection $Q_1 f$ contains the difference or *detail* information, illustrated in Fig. 8. Note that this does indeed represent Haar wavelets at level 1.

To see how the general decomposition emerges, consider

$$V_0 = V_1 \oplus W_1 = V_2 \oplus W_2 \oplus W_1 = V_3 \oplus W_3 \oplus W_2 \oplus W_1$$

This could be extended as far as desired. The general formula is

$$V_j = V_j \oplus \bigoplus_{k=0}^{J-j-1} W_{J-k} \tag{9}$$

where all subspaces on the right are orthogonal. This means that any function can be represented as a sum of detail parts plus a smoothed version of the original function. This is often expressed by saying that the function is resolved into a low-frequency part plus a sum of high-frequency parts. To see this, think of Fourier transforms. The broad part in V_J has a Fourier transform concentrated at the origin in the Fourier domain, hence low frequencies. The parts in W_j have Fourier transforms that must vanish at the origin since the area of the wavelet is 0, hence high-frequency parts.

By use of (M2) and Eq. (9) it follows that

$$L^2(\mathbb{R}) = \bigoplus_{j \in \mathbb{Z}} W_j \tag{10}$$

(Note that $V_j \to \{0\}$ as $j \to \infty$.) The collection $\{\psi_{j,k}; j, k \in \mathbb{Z}\}$ is an orthonormal basis for $L^2(\mathbb{R})$. The spaces W_j also have the scaling property (M3), so the job is to find a $\psi \in W_0$ such that the $\psi(x-k)$ form an orthonormal basis for W_0.

Orthonormal Wavelets with Compact Support

Before we embark on the task of determining other acceptable scaling and wavelet functions it may be useful to examine the Haar system more closely. Keep in mind that what we are doing applies to any functions ϕ and ψ that satisfy the multiresolution analysis and decomposition, Eq. (9).

First, we observe that the scaling function $\phi_{j,k}$ from Eq. (5) satisfies an orthogonality condition at the same scale,

$$\langle \phi_{j,k}, \phi_{j,k'} \rangle \equiv \int_{\mathbb{R}} \phi_{j,k}\phi_{j,k'}\,dx = \delta_{kk'} \tag{11}$$

Here $\delta_{kk'}$ is the Kronecker delta defined to be 1 if $k = k'$ and 0 if $k \neq k'$. The wavelets are orthogonal at the same scale and across scales,

$$\langle \psi_{j,k}, \psi_{j',k'} \rangle = \delta_{jj'}, \delta_{kk'} \quad (12)$$

The wavelets and scaling functions also satisfy

$$\langle \phi_{j,k}, \psi_{j',k'} \rangle = 0 \quad (13)$$

We focus our attention on the containment $V_0 \subset V_{-1}$ and $W_0 \subset V_{-1}$ for the Haar system,

$$\phi(x) = \phi(2x) + \phi(2x - 1) \quad \psi(x) = \phi(2x) - \phi(2x - 1)$$

This is a special case of general expansions for ϕ or ψ where

$$\phi(x) = \sum_{k\in\mathbb{Z}} c_k \phi(2x - k) \quad \psi(x) = \sum_{k\in\mathbb{Z}} d_k \phi(2x - k) \quad (14)$$

For the Haar system there are only two coefficients needed; namely, $c_0 = c_1 = 1$. The d coefficients are found from these. We will see later that the condition is $d_k = (-1)^k c_{1-k}$. One way to obtain the coefficients for more general functions ϕ and ψ is to place constraints on the coefficients c_k in the expansion of the scaling function. The method here follows the pioneer work on this by Ingrid Daubechies (30).

The expansion for $\phi(x)$ in Eq. (14) is called a *dilation equation*. If only a finite number of the coefficients are nonzero, then ϕ must vanish outside a finite interval. This gives the property of *compact support*. Suppose the nonzero coefficients are $c_m, c_{m+1}, \ldots, c_n$. If the original function ϕ has support on the interval $[a, b]$, then $\phi(2x)$ has support on the interval $[a/2, b/2]$. The shifted function $\phi(2x - k)$ has support on $[a + k/2, b + k/2]$. Since the index k goes from m to n we have

$$\phi(x) = \sum_{k=m}^{n} c_k \phi(2x - k) \quad (15)$$

The support on the left side is related to the support on the right side by

$$[a, b] = \left[\frac{a+m}{2}, \frac{b+n}{2}\right]$$

This requirement yields $a = m$ and $b = n$, hence the support is on $[m, n]$.

Example: Suppose $\phi(x)$ is the level 0 Haar box function, and let the sum go from 0 to n. If this function is substituted and used on the right side of Eq. (15) then the function on the left has support on $[0, 1 + n/2]$. If this function is now substituted on the right side the function on the left has support on $[0, 1 + 3n/4]$. If this procedure is continued the limiting case is just the interval $[0, n]$.

A *consistency condition* can be established by integrating the dilation equation. This is easy and the details that involve a change of variables ($t = 2x - k$) are left for the reader,

$$\int_{-\infty}^{\infty} \phi(x)\,dx = \int_{-\infty}^{\infty} \sum_k c_k \phi(2x-k)\,dx = \cdots = \frac{1}{2}\sum_k c_k \int_{-\infty}^{\infty} \phi(t)\,dt$$

Since the integral of the scaling function is assumed to be finite there is a requirement that

$$\sum_k c_k = 2 \quad (16)$$

A convenient choice for the normalization on ϕ is such that

$$\int_{-\infty}^{\infty} \phi(x)\,dx = 1$$

Caution: Some authors use a slightly different convention for the constants. The other popular choice is to use $c_n = \sqrt{2}\, h_n$, where h_n corresponds to the notation used by Daubechies (29).

The *orthogonality* condition in Eq. (11) leads to another important relation. The reader may wish to see Alpert (35) for details.

$$\begin{aligned}
\delta_{kl} &= \int_{-\infty}^{\infty} \phi(x-k)\phi(x-l)\,dx \\
&= \int_{-\infty}^{\infty} \sum_m c_m \phi[2(x-k)-m] \sum_n c_n \phi[2(x-l)-n]\,dx \\
&= \frac{1}{2}\sum_{m,n} c_m c_n \delta_{2k+m,2l+n} \\
&= \frac{1}{2}\sum_m c_m c_{2k-2l+m}
\end{aligned}$$

Since the sum is over all $m \in \mathbb{Z}$ we can make the change of index $m \to m + 2l$. This leads to the desired orthogonality condition

$$\sum_{m\in\mathbb{Z}} c_{2k+m} c_{2l+m} = 2\delta_{kl} \quad (17)$$

This equation ensures the orthogonality of the translates of the scaling function.

The coefficients d_k must be selected so that an orthogonality condition holds for the translates of the wavelet function $\psi(x)$. It is easy to show that this works for

$$d_k = (-1)^k c_{1-k} \quad (18)$$

The calculation makes use of Eqs. (14) and (17)

$$\begin{aligned}
&\int_{-\infty}^{\infty} \psi(x-k)\psi(x-l)\,dx \\
&= \sum_{m,n} \int_{-\infty}^{\infty} d_m \phi[2(x-k)-m] d_n \phi[2(x-l)-n]\,dx \\
&= \frac{1}{2}\sum_m d_{2k+m} d_{2l+m} \\
&= \frac{1}{2}\sum_m (-1)^{2k+m} c_{1-2k-m} (-1)^{2l+m} c_{1-2l-m} \\
&= \frac{1}{2}\sum_m c_{1-2k-m} c_{1-2k-l} \\
&= \delta_{kl}
\end{aligned}$$

Also, the choice made in Eq. (18) is adequate to establish the orthogonality

$$\int_{-\infty}^{\infty} \phi(x-k)\psi(x-l)\,dx = 0$$

This is left as an exercise; observe that you do not have to make use of Eq. (17).

The key conditions thus far are Eqs. (16), (17), and (18). These are not adequate for a unique determination of the coefficients that lead to the family of Daubechies that extend the Haar system in a natural way. The next condition relates to *approximation.*

The idea is to approximate polynomials of degree $j = 0, 1, \ldots, N-1$ as linear combinations of translates of the scaling function in V_0. Thus, we look for coefficients α such that

$$x^j = \sum_{k\in\mathbb{Z}} \alpha^N_{j,k}\phi(x-k), \quad (j = 0, 1, \ldots, N)$$

By orthogonality

$$\alpha^N_{j,k} = \int_{-\infty}^{\infty} x^j \phi(x-k)\,dx$$

The scaling function depends on N and is often written as $_N\phi$. Here we suppress the N and just use ϕ. Recall that only two coefficients are needed for the Haar scaling function. In this case polynomials of degree $N = 0$ can be represented with no error by scaling functions in V_0. For many situations as smoother scaling function is desired. We are looking for the conditions that must hold when we allow more than two coefficients, and require that polynomials of higher degree be represented exactly by functions in V_0.

The space V_0 is orthogonal to W_0; consequently, for $j = 0, \ldots, N-1$,

$$\int_{-\infty}^{\infty} x^j \psi(x)\,dx = 0$$

Now, use Eq. (14) along with the trick (identity)

$$x^j = \left(\frac{2x-k+k}{2}\right)^j$$

This yields

$$\int_{-\infty}^{\infty} \sum_k \left(\frac{2x-k+k}{2}\right)^j d_k\phi(2x-k)\,dx = 0$$

The general binomial expansion

$$(a+b)^j = \sum_{r=0}^{j} \binom{j}{r} a^{j-r}b^r, \quad \binom{j}{r} = \frac{j!}{r!(j-r)!}$$

can be applied to give

$$2^{-j}\sum_{r=0}^{j}\binom{j}{r}\sum_k k^{j-r}d_k\int_{-\infty}^{\infty}(2x-k)^r\phi(2x-k)\,dx = 0$$

The change of variables $2x - k \to x$ leads to

$$2^{-j-1}\sum_{r=0}^{j}\binom{j}{r}\sum_k k^{j-r}d_k\int_{-\infty}^{\infty}x^r\phi(x)\,dx = 0$$

The integral over x cannot be zero since by assumption x^r can be written as a linear combination of translates of ϕ for $r = 0, \ldots, N-1$. It follows that we must require

$$\sum_{r=0}^{j}\binom{j}{r}\sum_k k^{j-r}d_k = 0$$

hold for individual values of j from 0 to $N-1$. If you write this out for $j = 0$ then for $j = 1$, and $j = 2$ you see that the condition is

$$\sum_k k^j d_k = 0, \quad (j = 0, \ldots, N-1)$$

This is usually written in terms of the c_j coefficients from Eq. (18) with a slight modification. The index is usually shifted so the nonzero coefficients range from 0 to $2N-1$ for the Daubechies coefficients (29). This is accomplished by using the connection

$$d_k = (-1)^k c_{2N-1-k}$$

Then, the approximation condition becomes

$$\sum_{k=0}^{2N-1}(-1)^k k^j c_{2N-1-k} = 0, \quad (j = 0, \ldots, N-1) \tag{19}$$

Examples. The key equations are Eqs. (17)–(19). There are two coefficients for $N = 1$ that satisfy the conditions

$$c_0^2 + c_1^2 = 2, \quad c_0 - c_1 = 0$$

with region of support [0, 1]. These are the familiar Harr coefficients $c_0 = c_1 = 1$. For $N = 2$ we have four coefficients, known as the D4 coefficients. They satisfy orthogonality conditions

$$c_0^2 + c_1^2 + c_2^2 + c_3^2 = 2 \quad \text{and} \quad c_0c_2 + c_1c_3 = 0$$

and approximation conditions (for $j = 0$ and $j = 1$)

$$c_3 - c_2 + c_1 - c_0 = 0 \quad \text{and} \quad 0c_3 - 1c_2 + 2c_1 - 3c_0 = 0$$

The solution is unique up to a left–right reversal ($c_0 \leftrightarrow c_3$, $c_1 \leftrightarrow c_2$)

$$c_0 = (1+\sqrt{3})/4 \quad c_1 = (3+\sqrt{3})/4$$
$$c_2 = (3-\sqrt{3})/4 \quad c_3 = (1-\sqrt{3})/4$$

Note that Eq. (16) is also satisfied by these D4 coefficients. Keep in mind that if the other popular normalization condition is used $c_n = \sqrt{2}\,h_n$, then each of these coefficients must be divided by $\sqrt{2}$. When this is done then the sum of the squares is 1 rather than 2.

The region of support for the D4 scaling function and the wavelet function is [0, 3]. The graphs of these are shown in

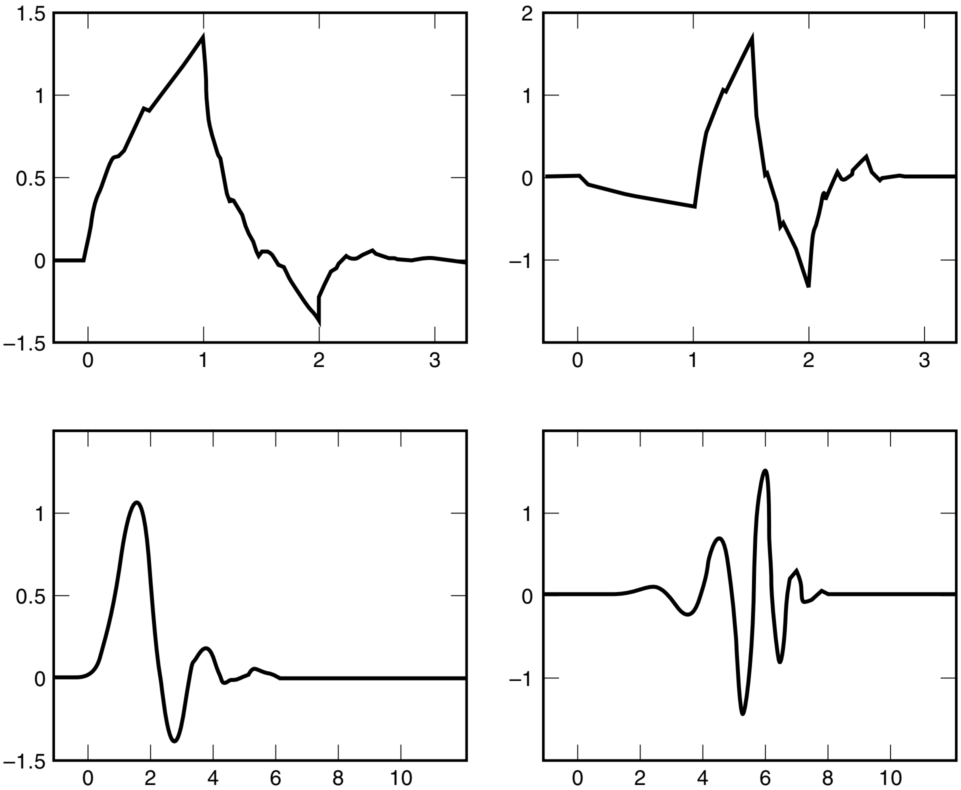

Figure 9. D4 scaling function (top left), D4 wavelet (top right), D12 scaling function (bottom left), and D12 wavelet (bottom right).

Fig. 9 across the top. The graphs for $N = 6$ (D12) are shown across the bottom. Here the region of support is [0, 11]. Note that as the number of coefficients increases the graphs get smoother and the region of support increases. Tables of coefficients for various values of N are given by Daubechies (29).

The functions in Fig. 9 are interesting, but knowing what these functions look like is absolutely unnecessary for implementation of the wavelet transform. The coefficients are all you need, coupled with an algorithm. An example is given in the section on *Mechanics of Doing Transforms,* and a method for obtaining Fig. 9 is indicated.

Other Wavelets. We have only touched the surface by indicating how to find the family of Daubechies wavelets. If the orthogonality and approximation conditions are modified, other sets of coefficients follow. For example, if you impose conditions of vanishing moments on ϕ as well as ψ then the resulting wavelets are known as *coiflets,* after a suggestion by Ronald R. Coifman of Yale University. For more information on these see Refs. 29, 36, and 37. Another example is provided by *biorthogonal wavelets.* The filter coefficients for the reconstruction are not the same as those for the decomposition, and there are two dual wavelet bases associated with two different multiresolution ladders. This leads to symmetric wavelets that are an advantage for some applications. Important references on these are by Cohen and Daubechies (38): Cohen, Daubechies, and Feauveau (39): and Vetterli and Herley (40).

Fourier Space Methods. Very powerful methods for finding wavelet coefficients are provided by Fourier techniques. These techniques can be used to find the family of Daubechies wavelets; also, they form a foundation for finding wavelets with other important properties. Here, we only indicate how this can be started and then refer the reader to some excellent references where this approach is utilized.

Start with the dilation equation for the scaling function

$$\phi(x) = \sum_k c_k \phi(2x - k)$$

The Fourier transform of this equation is

$$\hat{\phi}(\xi) = \sum_k c_k \int_{-\infty}^{\infty} \phi(2x - k) e^{-i\xi x}\, dx$$

The change of variables $t = 2x - k$ gives

$$\hat{\phi}(\xi) = \frac{1}{2} \sum_k c_k e^{-ik\xi/2} \int_{-\infty}^{\infty} \phi(t) e^{-i\xi t/2}\, dt$$

Observe that the integral is just $\hat{\phi}(\xi/2)$. This yields

$$\hat{\phi}(\xi) = m_0\left(\frac{\xi}{2}\right)\hat{\phi}\left(\frac{\xi}{2}\right)$$

where, in keeping with the notation of Daubechies (29), we define

$$m_0(\xi) \equiv \frac{1}{2}\sum_k c_k e^{-ik\xi}$$

Note that $m_0(0) = 1$ follows from

$$m_0(0) = \frac{1}{2}\sum_k c_k e^0 = \frac{1}{2}\sum_k c_k = 1$$

If we make the replacement $\xi \to \xi/2$ then

$$\hat{\phi}\left(\frac{\xi}{2}\right) = m_0\left(\frac{\xi}{4}\right)\hat{\phi}\left(\frac{\xi}{4}\right)$$

and

$$\hat{\phi}(\xi) = m_0\left(\frac{\xi}{2}\right)m_0\left(\frac{\xi}{4}\right)\hat{\phi}\left(\frac{\xi}{4}\right) = \left[\prod_{j=1}^{2} m_0\left(\frac{\xi}{2^j}\right)\right]\hat{\phi}\left(\frac{\xi}{2^2}\right)$$

Clearly this procedure can be continued to give

$$\hat{\phi}(\xi) = \left[\prod_{j=1}^{N} m_0\left(\frac{\xi}{2^j}\right)\right]\hat{\phi}\left(\frac{\xi}{2^N}\right)$$

As $N \to \infty$, $\hat{\phi}(\xi/2^N) \to \hat{\phi}(0) = 1$, since the area under the scaling function is normalized to 1. This means that as $N \to \infty$ the infinite product goes to the Fourier transform of the scaling function,

$$\hat{\phi}(\xi) = \prod_{j=1}^{\infty} m_0\left(\frac{\xi}{2^j}\right)$$

Example. Let us investigate how this works for the box function, the scaling function for the Haar case. If $c_0 = c_1 = 1$, then

$$m_0\left(\frac{\xi}{2}\right) = \frac{1}{2}(1 + e^{-i\xi/2})$$

and

$$m_0\left(\frac{\xi}{2}\right)m_0\left(\frac{\xi}{4}\right) = \frac{1}{2^2}(1 + e^{-i\xi/2})(1 + e^{i\xi/4})$$
$$= \frac{1}{2^2}(1 + e^{-i\xi/4} + e^{-2i\xi/4} + e^{-3i\xi/4})$$

The part in parenthesis on the right is just the sum of $2^2 = 4$ terms of a geometric series where the first term is 1 and the ratio term r is $e^{-i\xi/4}$. The sum of n terms is given by $(1 - r^n)/(1 - r)$. Thus

$$m_0\left(\frac{\xi}{2}\right)m_0\left(\frac{\xi}{4}\right) = \frac{1}{2^2}\frac{1 - e^{i\xi}}{1 - e^{-i\xi/4}}$$

In the general case where there are 2^j terms, the result is

$$m_0\left(\frac{\xi}{2}\right)\ldots m_0\left(\frac{\xi}{2^j}\right) = \frac{1}{2^j}\frac{1 - e^{i\xi}}{1 - e^{-\xi/2^j}}$$

Now let $2^{-j} = x$, then

$$2^j(1 - e^{-i\xi/2^j}) = \frac{1 - \cos x\xi}{x} + i\,\frac{\sin x\xi}{x}$$

In the limit as $j \to \infty$, and $x \to 0$ we get $i\xi$. It follows that

$$\prod_{j=1}^{\infty} m_0\left(\frac{\xi}{2^j}\right) = \frac{1 - e^{-i\xi}}{i\xi}$$

This is just the Fourier transform of ϕ where ϕ is the box function,

$$\hat{\phi}(\xi) = \int_{-\infty}^{\infty}\phi(x)e^{-i\xi x}\,dx = \int_0^1 e^{-\xi x}\,dx = \frac{1 - e^{-i\xi}}{i\xi}$$

just as expected.

A rich resource of information about wavelets comes from using Fourier techniques. The books by Hernández and Weiss (10), Vetterli and Kovačević (23), Strang and Nguyen (41), and Daubechies (29) are excellent sources.

MECHANICS OF DOING THE TRANSFORM

This example of how the wavelet transform can be implemented using matrices will be of value to those who wish to acquire an intuitive understanding about how the transform works. This is for illustration only, since in practice efficient code may not be written in matrix form. This example is for the simplest case, the Haar; however, the extension to smoother cases is easy and we will indicate how following this example. The following operations are illustrated:

1. Generate the wavelet coefficients with down sampling.
2. Show how this is a dual filter operation with a shrinking matrix and signal.
3. Mechanics of the reconstruction, the inverse transform.

There is a pyramidal structure to the procedure. At each level the detail information is stored, while the smooth information may be transformed at the next higher scale. One way to indicate this is shown in Fig. 10, where we have carried the transform through three stages.

Let the transpose of the original signal vector for an eight-point transform be designated by

$$[16, 32, 64, 16, 6, 32, 16, 8]$$

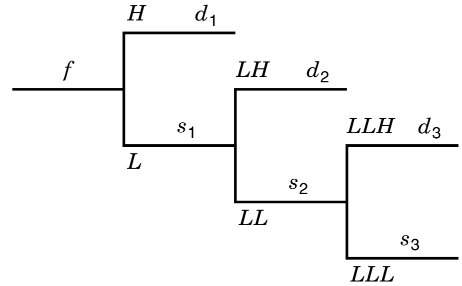

Figure 10. Pyramidal decomposition of a signal. The low- and high-pass parts are indicated by L and H. The corresponding smooth and detail parts are designated by s and d with subscripts indicating the level.

The full smoothing operator (the low pass part) with $c_0 = c_1 = 1$ is given by

$$S = \frac{1}{2}\begin{pmatrix} 1 & 1 & 0 & 0 & 0 & 0 & 0 & 0 \\ 0 & 1 & 1 & 0 & 0 & 0 & 0 & 0 \\ 0 & 0 & 1 & 1 & 0 & 0 & 0 & 0 \\ 0 & 0 & 0 & 1 & 1 & 0 & 0 & 0 \\ 0 & 0 & 0 & 0 & 1 & 1 & 0 & 0 \\ 0 & 0 & 0 & 0 & 0 & 1 & 1 & 0 \\ 0 & 0 & 0 & 0 & 0 & 0 & 1 & 1 \\ 1 & 0 & 0 & 0 & 0 & 0 & 0 & 1 \end{pmatrix}$$

The shift on the last row is to take into account edge effects, and is essential to insure that the inversion is exact. The highpass operator associated with the detail is given by

$$H = \frac{1}{2}\begin{pmatrix} 1 & -1 & 0 & 0 & 0 & 0 & 0 & 0 \\ 0 & 1 & -1 & 0 & 0 & 0 & 0 & 0 \\ 0 & 0 & 1 & -1 & 0 & 0 & 0 & 0 \\ 0 & 0 & 0 & 1 & -1 & 0 & 0 & 0 \\ 0 & 0 & 0 & 0 & 1 & -1 & 0 & 0 \\ 0 & 0 & 0 & 0 & 0 & 1 & -1 & 0 \\ 0 & 0 & 0 & 0 & 0 & 0 & 1 & -1 \\ -1 & 0 & 0 & 0 & 0 & 0 & 0 & 1 \end{pmatrix}$$

Now we calculate the detail and smooth coefficients that lie in W_1 and V_1, respectively

$$d_1 = Hf \downarrow = [-8, -16, 24, 4, -12, 8, 4, -4] \downarrow = [-8, 24, -12, 4]$$

and

$$s_1 = Sf \downarrow = [24, 48, 40, 12, 20, 24, 12, 12] \downarrow = [24, 40, 20, 12]$$

The use of the down arrow is to indicate down sampling. Every other value is discarded. You might think information has been lost by doing this, but note that you started with eight independent values in the signal and after down sampling you still have eight independent values, four detail and four smooth coefficients. These can be used to recover the original values. The next step is to contract the matrices S and H,

$$S = \frac{1}{2}\begin{pmatrix} 1 & 1 & 0 & 0 \\ 0 & 1 & 1 & 0 \\ 0 & 0 & 1 & 1 \\ 1 & 0 & 0 & 1 \end{pmatrix} \qquad H = \frac{1}{2}\begin{pmatrix} 1 & -1 & 0 & 0 \\ 0 & 1 & -1 & 0 \\ 0 & 0 & 1 & -1 \\ -1 & 0 & 0 & 1 \end{pmatrix}$$

The coefficients for W_2 and V_2 follow by applying these new contracted matrices to the s_1 vector,

$$d_2 = Hs_1 \downarrow = [-8, 10, 4, -6] \downarrow = [-8, 4]$$
$$s_2 = Ss_1 \downarrow = [32, 30, 16, 16] \downarrow = [32, 16]$$

Once again we contract S and H,

$$S = \frac{1}{2}\begin{pmatrix} 1 & 1 \\ 1 & 1 \end{pmatrix} \qquad H = \frac{1}{2}\begin{pmatrix} 1 & -1 \\ -1 & 1 \end{pmatrix}$$

The last two coefficients are found as before

$$d_3 = Hs_2 \downarrow = [8, -8] \downarrow = [8], \qquad s_3 = Ss_2 \downarrow = [24, 24] \downarrow = [24]$$

This completes the eight-point transform. The eight points in the signal vector have been transformed by the Haar wavelet transform to eight points,

$$d_1 = [-8, 24, -12, 4] \quad d_2 = [-8, 4] \quad d_3 = [8] \quad s_3 = [24]$$

The inverse transform must start with the wavelet coefficients and end with the original signal coefficients. This is done by a clever reversal of the directions in Fig. 10, with a sum used to go from two branches on the right to one on the left, at a vertex where three lines meet. Here is how it works. Use the transpose of S and H without the factor of $\frac{1}{2}$ at each step and insert zeros where there were discarded values. This upsampling is indicated by the up arrow.

$$S^\dagger = \begin{pmatrix} 1 & 1 \\ 1 & 1 \end{pmatrix} \qquad H^\dagger = \begin{pmatrix} 1 & -1 \\ -1 & 1 \end{pmatrix}$$
$$S^\dagger s_3 \uparrow = S^\dagger \begin{pmatrix} 24 \\ 0 \end{pmatrix} = \begin{pmatrix} 24 \\ 24 \end{pmatrix} \qquad H^\dagger d_3 \uparrow = H^\dagger \begin{pmatrix} 8 \\ 0 \end{pmatrix} = \begin{pmatrix} 8 \\ -8 \end{pmatrix}$$

The s_2 signal is recovered by addition

$$\begin{pmatrix} 24 \\ 24 \end{pmatrix} + \begin{pmatrix} 8 \\ -8 \end{pmatrix} = \begin{pmatrix} 32 \\ 16 \end{pmatrix}$$

At the next step we have

$$S^\dagger = \begin{pmatrix} 1 & 0 & 0 & 1 \\ 1 & 1 & 0 & 0 \\ 0 & 1 & 1 & 0 \\ 0 & 0 & 1 & 1 \end{pmatrix} \qquad H^\dagger = \begin{pmatrix} 1 & 0 & 0 & -1 \\ -1 & 1 & 0 & 0 \\ 0 & -1 & 1 & 0 \\ 0 & 0 & -1 & 1 \end{pmatrix}$$

$$S^\dagger s_2 \uparrow = S^\dagger \begin{pmatrix} 32 \\ 0 \\ 16 \\ 0 \end{pmatrix} = \begin{pmatrix} 32 \\ 32 \\ 16 \\ 16 \end{pmatrix}$$

$$H^\dagger d_2 \uparrow = H^\dagger \begin{pmatrix} -8 \\ 0 \\ 4 \\ 0 \end{pmatrix} = \begin{pmatrix} -8 \\ 8 \\ 4 \\ -4 \end{pmatrix}$$

Again by addition we recover the s_1 signal,

$$\begin{pmatrix} 32 \\ 32 \\ 16 \\ 16 \end{pmatrix} + \begin{pmatrix} -8 \\ 8 \\ 4 \\ -4 \end{pmatrix} = \begin{pmatrix} 24 \\ 40 \\ 20 \\ 12 \end{pmatrix}$$

In the final step we are back to the full matrices

$$S^\dagger = \begin{pmatrix} 1 & 0 & 0 & 0 & 0 & 0 & 0 & 1 \\ 1 & 1 & 0 & 0 & 0 & 0 & 0 & 0 \\ 0 & 1 & 1 & 0 & 0 & 0 & 0 & 0 \\ 0 & 0 & 1 & 1 & 0 & 0 & 0 & 0 \\ 0 & 0 & 0 & 1 & 1 & 0 & 0 & 0 \\ 0 & 0 & 0 & 0 & 1 & 1 & 0 & 0 \\ 0 & 0 & 0 & 0 & 0 & 1 & 1 & 0 \\ 0 & 0 & 0 & 0 & 0 & 0 & 1 & 1 \end{pmatrix}$$

$$H^\dagger = \begin{pmatrix} 1 & 0 & 0 & 0 & 0 & 0 & 0 & -1 \\ -1 & 1 & 0 & 0 & 0 & 0 & 0 & 0 \\ 0 & -1 & 1 & 0 & 0 & 0 & 0 & 0 \\ 0 & 0 & -1 & 1 & 0 & 0 & 0 & 0 \\ 0 & 0 & 0 & -1 & 1 & 0 & 0 & 0 \\ 0 & 0 & 0 & 0 & -1 & 1 & 0 & 0 \\ 0 & 0 & 0 & 0 & 0 & -1 & 1 & 0 \\ 0 & 0 & 0 & 0 & 0 & 0 & -1 & 1 \end{pmatrix}$$

The up sampling gives

$$S^\dagger s_1 \uparrow = S^\dagger \begin{pmatrix} 24 \\ 0 \\ 40 \\ 0 \\ 20 \\ 0 \\ 12 \\ 0 \end{pmatrix} = \begin{pmatrix} 24 \\ 24 \\ 40 \\ 40 \\ 20 \\ 20 \\ 12 \\ 12 \end{pmatrix} \qquad H^\dagger d_1 \uparrow = H^\dagger \begin{pmatrix} -8 \\ 0 \\ 24 \\ 0 \\ -12 \\ 0 \\ 4 \\ 0 \end{pmatrix} = \begin{pmatrix} -8 \\ 8 \\ 24 \\ -24 \\ -12 \\ 12 \\ 4 \\ -4 \end{pmatrix}$$

The original signal vector is recovered by addition

$$f = \begin{pmatrix} 24 \\ 24 \\ 40 \\ 40 \\ 20 \\ 20 \\ 12 \\ 12 \end{pmatrix} + \begin{pmatrix} -8 \\ 8 \\ 24 \\ -24 \\ -12 \\ 12 \\ 4 \\ -4 \end{pmatrix} = \begin{pmatrix} 16 \\ 32 \\ 64 \\ 16 \\ 8 \\ 32 \\ 16 \\ 8 \end{pmatrix}$$

This concludes the Haar example; however, some additional things should be observed. It is possible to combine the matrix multiplication and the up and down sampling. For a discussion of this see Strang and Nguyen (41). Also, one can combine the operations of finding the d and s parts along with the down sampling. A practical example of this is contained in Ref. 42, section 13.10, for the Daubechies D4 wavelet with four coefficients. In addition to Ref. 42 other sources of code for efficient implementation of the forward and inverse wavelet transform include Bruce and Gao (43), and Cody (44,45). Also, see the section on Wavelet Resources on the Internet. Finally, note that if we start with

$$d_1 = [0, 0, 0, 0] \qquad d_2 = [0, 0] \qquad d_3 = [1] \qquad s_3 = [0]$$

and apply the inverse transform we get back the wavelet function

$$[1, 1, 1, 1, -1, -1, -1, -1]$$

This is one way to obtain the wavelets illustrated in Fig. 9. We simply run a unit vector, made up of 0's except for a 1 in a single location through the inverse transform.

OCTAVE BAND TREE STRUCTURE

The type of division of the spectrum for the tree structure of Fig. 10 is known as a *dyadic* or *octave* band. The part labeled s is the low-pass part and the part labeled d is the high-pass part. At each level of the tree the lower half of the spectrum is split into two equal bands. In Fourier space this can be represented by Fig. 11. For an extensive discussion of tree structures and the corresponding frequency band splits, see Akansu and Haddad (46). Another important type of tree structure for wavelet analysis is that used in connection with wavelet packets and best basis algorithms pioneered by Coifman and Wickerhauser (47,48) and Wickerhauser (49). In this type of tree there is an option along both the high-pass and low-pass branches to send the signal through more high-pass and low-pass filters. This is part of an important and extensive area of wavelet theory known as *adaptive wavelet transform methods.* For a full discussion we refer the reader to Refs. 47–49 and the Reading List.

An extension of the octave band tree structure to 2-D was suggested by Burt and Adelson (24). The technique goes by the name of the *Laplacian pyramid.* The multiresolution analysis can be extended to 2-D for functions $f(x, y)$, for details see Daubechies (29). We define a scaling function of two variables and three wavelets. These come from tensor products of horizontal and vertical 1-D wavelets. Here superscripts s, h, v, and d refer to smooth, horizontal, vertical, and diagonal, respectively.

$$\begin{aligned} \Phi^s(x, y) &= \phi(x)\phi(y) \quad L(x)L(y) \\ \Psi^h(x, y) &= \phi(x)\psi(y) \quad L(x)H(y) \\ \Psi^v(x, y) &= \psi(x)\phi(y) \quad H(x)L(y) \\ \Psi^d(x, y) &= \psi(x)\psi(y) \quad H(x)H(y) \end{aligned}$$

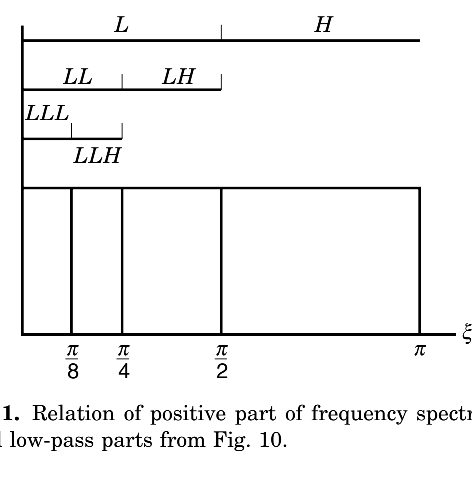

Figure 11. Relation of positive part of frequency spectrum to ideal high- and low-pass parts from Fig. 10.

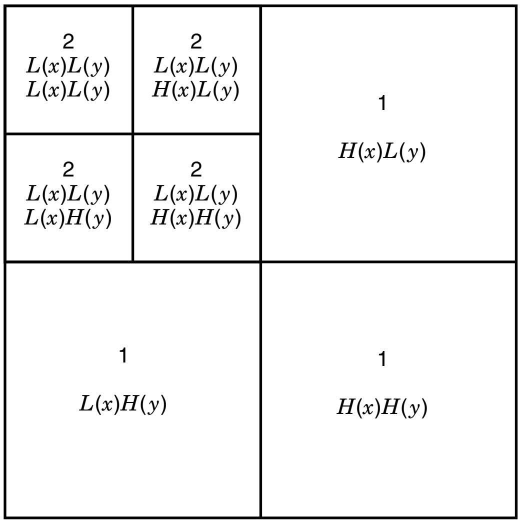

Figure 12. Decomposition of the 2-D transform into two levels. To go to the next level the low-pass part in the upper left is further broken down just as going from level 1 to level 2.

This leads to a decomposition at levels 1 and 2 illustrated by Fig. 12. At level 2 the smooth part from level 1 is further divided to produce the parts in the upper left corner. To go to level 3 the upper left smooth–smooth part would be further broken down as in going from level 1 to level 2. This can go on as far as is practical. In an image, horizontal edges show prominently in the Ψ^h part, vertical edges in the Ψ^v part, and diagonal edges in the Ψ^d part. See Fig. 13 and the discussion and images in Chapter 10 of Ref. 29.

SOME INTERESTING APPLICATIONS

The range of fields, both pure and applied, where wavelets have had an impact is wide. The disciplines include mathematics, physics, geophysics, fluid dynamics, engineering, computer science, and medicine. The broad list of topics include Fourier analysis, approximation theory, numerical analysis, functional analysis, operator theory, group representations, fractals, turbulence, signal processing, image processing, medical imaging, various types of compressions, speech and audio, image, and video. In this section we give a brief introduction to some of these applications and provide the reader with references to current literature for further study.

Compression

In many cases a digitized image contains more information than is needed to convey the message the image carries. In these cases we want to remove some of the information in the original image without degrading the quality too much; this is called *lossy compression.* This modified image can be stored more economically and can be transmitted more rapidly, using less bandwidth over a communications channel. Wavelets have been used for these kinds of problems with striking success. We illustrate this in Fig. 14. The original image is upper left. To obtain the image upper right we performed a wavelet transform of the original image, kept 25% of the coefficients with the largest magnitude, replaced the other 75% with zeros, then did the inverse transform. The resulting image is clearly degraded, but not significantly. On the lower left we did the same thing with 6.25% of the coefficients, and on the lower right with only 1.56%.

There is an enormous amount of literature on compression. Here we suggest only a few recent articles. These contain guidance to earlier work. Uses of wavelet transform maxima in signal and image processing are described by Mallat and Zhong (50) and Mallat (51). Some new ideas on optimal compression are discussed by Hsiao, Jawerth, Lucier, and Yu (52) and DeVore, Jawerth, and Lucier (53). See Ref. 23 for a general discussion of video compression, and speech and audio compression. Acoustic signal compression with wavelet packets and a comparison of compression methods are given by Wickerhauser (54,55), and some general theorems on optimal bases for data compression are developed by Donoho (56).

Turbulence

Wavelet analysis has provided a new means for examining the structure of turbulent flow. They are especially useful when it is important to obtain some information about the spatial structure of the flow. Some of the pioneer work in this area along with a comparison of older methods is in the review by Marie Farge (57). Also, see the paper on wavelets and turbulence by Farge, Kevlahan, Perrier, and Goirand (58) for a discussion of the main applications of wavelets and wavelet packets to analyze, model, and compute turbulent flows. Wavelet spectra of buoyant atmospheric turbulence are analyzed by Mayer, Hudgins, and Friehe (59) and an experimen-

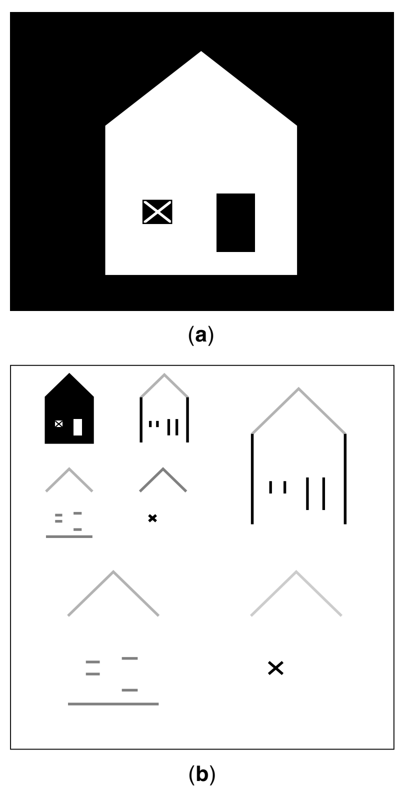

Figure 13. (a) House to be decomposed using wavelet transform. (b) Decomposition through level 2. The gray scale has been reversed and rescaled to emphasize the important features. Note the prominence of the vertical, horizontal, and diagonal parts in the appropriate locations.

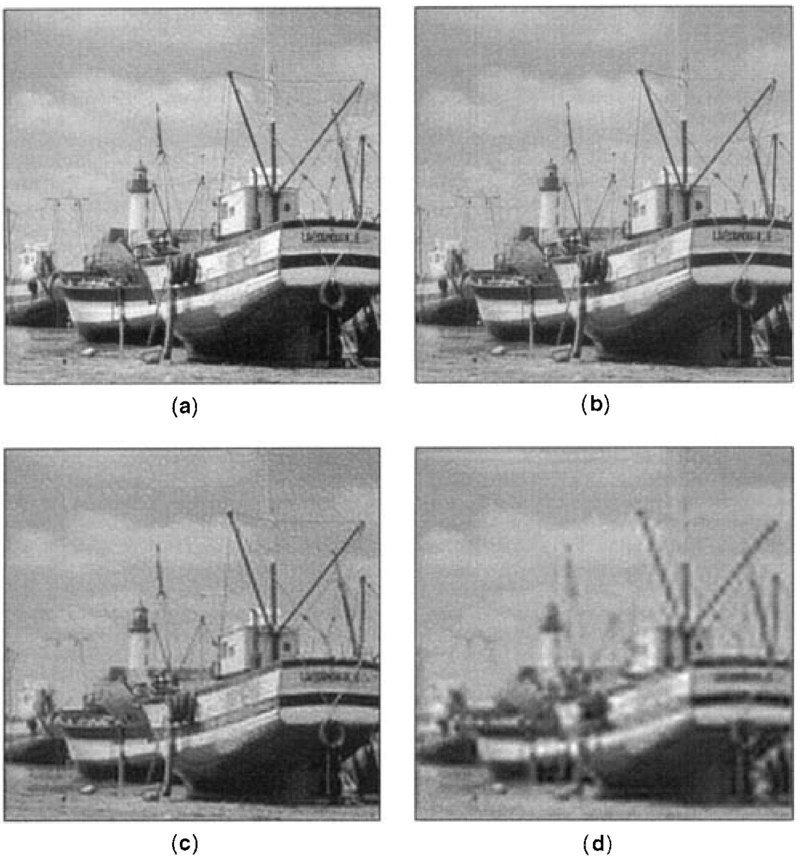

Figure 14. Boat figure to illustrate compression: (a) original, (b) use largest 25%, (c) use largest 6.25%, (d) use largest 1.56%. The degradation can be seen as fewer and fewer coefficients are used to reconstruct the boat.

tal study of inhomogeneous turbulence in the lower troposphere using wavelet analysis is discussed by Druilhet et al. (60). Wickerhauser et al. (61) compare methods for compression of a two-dimensional turbulent flow, and find that the wavelet packet representation is superior to the local cosine representation.

Fractals

The wavelet transform is valuable for the efficient representation of scale-invariant signals. Fractal geometry is being used more and more to describe processes that do not fit naturally into traditional Euclidean geometry. Many fractals of interest have structure that is *similar* on different scales. These properties of wavelets and fractals lead to important foundations for scale-invariant signal models. The discrete wavelet transform algorithm is a key component for practical processing of scale-invariant signals, and for estimating fractal dimensions. Signal processing with fractals using wavelets is an emerging area, one that is exciting with much work remaining to be done. An important resource in this field is the book by Wornell (62). The local self-similarity aspect of fractals and the analysis through wavelet transforms is discussed by Holschneider (34), Chapter 4. These two references and the brief review by Hazewinkel (63) provide guidance to the rich literature in this field.

Medicine and Biology

Wavelets are playing an important role in many areas of medicine and biology. A review of one-dimensional processing in bio-acoustics, electrocardiography (ECG), and electroencephalography (EEG) is given by Unser and Aldroubi (64). This article also contains a brief review of biomedical image processing. Applications of importance include: *noise reduction* in magnetic resonance images (65) using methods systematized by Donoho and Johnstone (66,67) and DeVore and Lucier (68), *image enhancement and segmentation* in digital mammography to accentuate and detect image features that are clinically relevant (69–71), and *image restoration* to restore degradation due to photon scattering and collimator photon penetration with the gamma camera (72). A general strategy for extraction of microcalcification clusters in digitized mammograms making use of wavelets is outlined by DeVore, Lucier, and Yang (73), and a multiresolution statistical method for the identification of normal mammograms with respect to microcalcifications has been developed (74); the key to the method is the recognition of the statistical properties of the various levels of the wavelet decomposition. In *computer-assisted tomography* (CT) the Radon transform (75) is fundamental to the algorithms for reconstruction from projections. Several authors have successfully combined wavelet methods with Radon methods to obtain improved algorithms for certain areas of CT (see Refs. 64 and 76 and citations therein). Other medical applications are to *magnetic resonance imaging* (MRI) (77) and functional neuroimaging using *positron emission tomography* (PET) and *functional MRI* (fMRI). A review is given by Unser and Aldroubi (64).

Others

There are several other areas of application where the wavelet transform plays a key role. We have added a reading list at the end of the bibliography. A quick survey of this list will provide guidance to good starting points for various applications.

WAVELETS ON THE INTERNET

An increasing amount of wavelet resources are available on the Internet. Preprints of academic papers are available on the Internet long before they appear in print. Many researchers maintain Internet sites where they post their papers, software, and tutorial guides. In fact the World Wide Web (Web), the graphical interface of the Internet, was created by Tim Berners-Lee while he was at the CERN particle physics laboratory in Geneva. The particle physics community has pioneered in the use of the Internet and the Web in the exchange of ideas, abstracts, and papers since 1991.

A similar effort has been made by Wim Sweldens who founded the *Wavelet Digest* in 1992. The *Wavelet Digest* is a free monthly newsletter, edited by Sweldens, available to subscribers by e-mail. One can browse through past issues of the digest at the Wavelet Digest home page (http://www.wavelet.org/wavelet/index.html). The *Wavelet Digest* carries announcements of papers, books, conferences, and seminars in the field of wavelets. It is also a forum for subscribers to ask questions they have about wavelets. Given the wide reach of the *Wavelet Digest* someone is likely to have an answer for almost any question.

The Collection of Computer Science Bibliographies at the Department of Computer Science of the University of Karlsruhe, Germany has a *Bibliographies on Wavelets* (http://liinwww.ira.uka.de/bibliography/Theory/Wavelets/). This is a fairly comprehensive collection of references, although many of them are not available on the Web.

The MathSoft Wavelet Resources page (http://www.mathsoft.com/wavelets.html) has a list of links to preprints and papers available on the Web.

Most wavelet pages on the Web have links to other wavelet resources on the Web. The wavelet page maintained by Andreas Uhl at the Department of Mathematics at the University of Salzburg, Austria (http://www.mat.sbg.ac.at/~uhl/wav.html) has a useful list of links to wavelet pages, and the Amara Graps wavelet page (http://www.amara.com/current/wavelet.html) has a comprehensive list of wavelet links. Also the Amara Graps page provides a list of wavelet software available on the Internet along with a brief description of each software listed.

The WaveLab software for Matlab written by David Donoho, Iain Johnstone, Jonathan Buckheit, and Shaobing Chen at the Stanford University Statistics Department along with Jeffrey Scargle at NASA-Ames Research Center is available at (http://stat.stanford.edu/~wavelab/). This site includes Macintosh, Unix, and PC versions of the software including instructions on how to download and install the software.

MathWorks, the creators of Matlab, have introduced the Wavelet Toolbox. The Wavelet Toolbox is written by Michael Misiti, Yves Misiti, Georges Oppenheim, and Jean-Michel Poggi, who are all members of "Laboratoire de Mathmatiques," Orsay-Paris 11 University, France. The book *Wavelets and Filter Banks,* by Gilbert Strang and Truong Nguyen (41), comes with the Toolbox. The exercises and examples in the book complement the Wavelet Toolbox. The Toolbox has both graphical user interface (GUI) and command line routines. Information on the toolbox can be found at the Matlab Wavelet Toolbox site (http://www.mathworks.com/products/wavelettbx.shtml).

An example of a wavelet application in the real world can be found at the Federal Bureau of Investigation (FBI) fingerprint image compression standard website (http://www.c3.lanl.gov/~brislawn/FBI/FBI.html). The FBI selected a wavelet standard for digitized fingerprints, and this site gives some of the reasons behind the choice.

Another interesting site on the Web is the Jelena Kovačević Bell Labs Wavelet Group page which includes a link to wavelet related Java applets (http://cm.bell-labs.com/who/jelena/Wavelet/w_applets.html).

This list is far from comprehensive. The interested reader can find wavelet-related links at these sites or by searching on any of the Internet search engines. There are some things one must keep in mind while browsing the Web. Not all information on the Web has been screened by any rigorous peer-review process. One must check the provenance of the information on the Web. Also note that Web addresses are not permanent. The author of a page may graduate or change jobs and the site could be removed. The Internet is a useful resource for any serious researcher. One cannot only get a lot of useful information on the Web, but one can contact other researchers to exchange ideas, data, and programs.

BIBLIOGRAPHY

1. R. N. Bracewell, *The Fourier Transform and Its Applications,* 3rd ed., New York: McGraw-Hill, 1986.
2. E. O. Brigham, *The Fast Fourier Transform and Its Applications,* Engelwood Cliffs, NJ: Prentice-Hall, 1988.
3. M. T. Heideman, D. H. Johnson, and C. S. Burrus, Gauss and the history of the fast Fourier transform, *IEEE Acoust. Speech Signal Process. Mag.,* **1** (4): 14–21, 1984.
4. D. Gabor, Theory of communication, *J. IEE,* **93**: 429–457, 1946.
5. O. Rioul and M. Vetterli, Wavelets and signal processing, *IEEE Signal Process. Mag.,* **8** (4): 14–38, October 1991.
6. B. B. Hubbard, *The World According to Wavelets,* Wellesley, MA: A K Peters, 1996.
7. Y. Meyer, *Wavelets Algorithms & Applications,* Philadelphia: SIAM, 1993.
8. A. Haar, Zur theorie der orthogonalen funktionen-systeme, *Math. Ann.,* **69**: 331–371, 1910.
9. P. Franklin, A set of continuous orthogonal functions, *Math. Ann.,* **100**: 522–529, 1928.
10. E. Hernández and G. Weiss, *A First Course on Wavelets,* Boca Raton, FL: CRC Press, 1996.
11. R. E. Edwards and G. I. Gaudry, *Littlewood-Paley and Multiplier Theory,* Berlin: Springer-Verlag, 1977.
12. E M. Stein, *Harmonic Analysis: Real-Variable Methods, Orthogonality, and Oscillatory Integrals,* Princeton, NJ: Princeton University Press, 1993.
13. J.-O. Strömberg, A modified Franklin system and higher-order spline systems on $\mathbb{R}^n$ as unconditional bases for Hardy spaces, in W. Beckner et al. (eds.), *Conference on Harmonic Analysis in Honor of Antoni Zygmund,* Belmont CA: Wadsworth, 1983, vol. 2, pp. 475–494.
14. K. G. Wilson, Renormalization group and critical phenomens, II, Phase-space cell analysis of critical behavior, *Phys. Rev. B,* **4**: 3184–3205, 1971.

15. G. Battle, Wavelets: A renormalization group point of view, in M. B. Ruskai et al. (eds.), *Wavelets and Their Applications,* Boston: Jones and Bartlett, 1992, pp. 323–349.

16. G. Battle, Wavelet refinement of the Wilson recursion formula, in L. L. Schumaker and G. Webb (eds.), *Recent Advances in Wavelet Analysis,* San Diego: Academic Press, 1994, pp. 87–118.

17. R. J. Glauber, Coherent and incoherent states of the radiation field, *Phys. Rev.,* **131**: 2766–2788, 1963.

18. E. W. Aslaksen and J. R. Klauder, Unitary representations of the affine group, *J. Math. Phys.,* **9**: 206–211, 1968.

19. E. W. Aslaksen and J. R. Klauder, Continuous representation theory using the affine group, *J. Math. Phys.,* **10**: 2267–2275, 1969.

20. A. Crosier, D. Esteban, and C. Galand, Perfect channel splitting by use of interpolation/decimation/tree decomposition techniques, *Int. Conf. Inform. Sci. Syst.,* Patras, Greece, 1976, pp. 443–446.

21. D. Esteban and C. Galand, Application of quadrature mirror filters to split band voice coding schemes, *Proc. IEEE Int. Conf. Acoust. Speech Signal Process.,* 1977, pp. 191–195.

22. R. E. Crochiere, S. A. Webber, and J. L. Flanagan, Digital coding of speech sub-bands, *Bell Syst. Tech. J.,* **55**: 1069–1085, 1976.

23. M. Vetterli and J. Kovačević, *Wavelets and Subband Coding,* Englewood Cliffs, NJ: Prentice-Hall, 1995.

24. P. J. Burt and E. H. Adelson, The Laplacian pyramid as a compact image code, *IEEE Trans. Commun.,* **31**: 532–540, 1983.

25. J. Morlet et al., Wave propagation and sampling theory—Part II: Sampling theory and complex waves, *Geophysics,* **47**: 222–236, 1982.

26. A. Grossmann and J. Morlet, Decomposition of Hardy functions into square integrable wavelets of constant shape, *SIAM J. Math. Anal.,* **15**: 723–736, 1984.

27. S. G. Mallat, A theory for multiresolution signal decomposition: The wavelet representation, *IEEE Trans. Pattern Anal. Mach. Intell.,* **11**: 674–693, 1989.

28. S. G. Mallat, Multiresolution approximations and wavelet orthogonal bases of $L^2(\mathbb{R})$, *Trans. Amer. Math. Soc.,* **315**: 69–87, 1989.

29. I. Daubechies,, *Ten Lectures on Wavelets,* Philadelphia: SIAM, 1992.

30. I. Daubechies, Orthonormal bases of compactly supported wavelets, *Comm. Pure Appl. Math.,* **41**: 909–996, 1988.

31. I. Daubechies, The wavelet transform, time-frequency localization and signal analysis, *IEEE Trans. Inf. Theory,* **36**: 961–1005, 1990.

32. I. Daubechies, Where do wavelets come from?—A personal point of view, *Proc. IEEE,* **84**: 510–513, 1996.

33. C. E. Heil and D. F. Walnut, Continuous and discrete wavelet transforms, *SIAM Rev.,* **31**: 628–666, 1989.

34. M. Holschneider, *Wavelets an Analysis Tool,* Oxford: Clarendon Press, 1995.

35. B. K. Alpert, Wavelets and other bases for fast numerical linear algebra, in C. K. Chui (ed.), *Wavelets: A Tutorial in Theory and Applications,* San Diego: Academic Press, 1992, pp. 181–216.

36. I. Daubechies, Orthonormal bases of compactly supported wavelets II. Variations on a theme, *SIAM J. Math. Anal.,* **24**: 499–519, 1993.

37. G. Beylkin, R. Coifman, and V. Rokhlin, Fast wavelet transforms and numerical algorithms I, *Comm. Pure Appl. Math.,* **44**: 141–183, 1991.

38. A. Cohen and I. Daubechies, A stability criterion for biorthogonal wavelet bases of compactly supported wavelets, *Duke Math. J.,* **68**: 313–335, 1992.

39. A. Cohen, I. Daubechies, and J.-C. Feauveau, Biorthogonal bases of compactly supported wavelets, *Comm. Pure Appl. Math.,* **45**: 485–560, 1992.

40. M. Vetterli and C. Herley, Wavelets and filter banks: Theory and design, *IEEE Trans. Signal Process.,* **40**: 2207–2232, 1992.

41. G. Strang and T. Nguyen, *Wavelets and Filter Banks,* Wellesley, MA: Wellesley-Cambridge Press, 1996.

42. W. H. Press et al., *Numerical Recipes in C,* 2nd ed., Cambridge: Cambridge University Press, 1992.

43. A. Bruce and H.-Y. Gao, *Applied Wavelet Analysis with S-PLUS,* New York: Springer, 1996.

44. M. A. Cody, The fast wavelet transform, *Dr. Dobb's J.,* **17** (4): 16–28, 1992.

45. M. A. Cody, The wavelet packet transform, *Dr. Dobb's J.,* **19** (4): 44–54, 1994.

46. A N. Akansu and R. A. Haddad, *Multiresolution Signal Decomposition,* San Diego: Academic Press, 1992.

47. R. R. Coifman and M. V. Wickerhauser, Entropy-based algorithms for best basis selection, *IEEE Trans. Inf. Theory,* **38**: 713–718, 1992.

48. R. R. Coifman and M. V. Wickerhauser, Wavelets and adapted waveform analysis, in J. J. Benedetto and M. W. Frazier (eds.), *Wavelets: Mathematics and Applications,* Boca Raton, FL: CRC Press, 1994, pp. 399–423.

49. M. V. Wickerhauser, *Adapted Wavelet Analysis from Theory to Software,* Wellesley, MA: A. K. Peters, 1994.

50. S. Mallat and S. Zhong, Wavelet transform maxima and multiscale edges, in M. B. Ruskai et al. (eds.), *Wavelets and Their Applications,* Boston: Jones and Bartlett, 1992, pp. 67–104.

51. S. Mallat, Wavelets for a vision, *Proc. IEEE,* **84**: 604–614, 1996.

52. C.-C. Hsiao et al., Near optimal compression of orthonormal wavelet expansions, in J. J. Benedetto and M. W. Frazier (eds.), *Wavelets: Mathematics and Applications,* Boca Raton, FL: CRC Press, 1994, pp. 425–446.

53. R. A. DeVore, B. Jawerth, and B. J. Lucier, Image compression throught wavelet transform coding, *IEEE Trans. Inf. Theory,* **38**: 719–746, 1992.

54. M. V. Wickerhauser, Acoustic signal compression with wavelet packets, in C. K. Chui (ed.), *Wavelets: A Tutorial in Theory and Applications,* San Diego: Academic Press, 1992, pp. 679–700.

55. M. V. Wickerhauser, Comparison of picture compression methods: Wavelet, wavelet packet, and local cosine transform coding, in C. K. Chui, L. Montefusco, and L. Puccio, (eds.), *Wavelets: Theory, Algorithms, and Applications,* San Diego: Academic Press, 1994, pp. 585–621.

56. D. L. Donoho, Unconditional bases are optimal bases for data compression and for statistical estimation, *Appl. Computat. Harmonic Anal.,* **1**: 100–115, 1993.

57. M. Farge, Wavelet transforms and their applications to turbulence, *Annu. Rev. Fluid Mech.,* **24**: 395–457, 1992.

58. M. Farge et al., Wavelets and turbulence, *Proc. IEEE,* **84**: 639–669, 1996.

59. M. E. Mayer, L. Hudgins, and C. A. Friehe, Wavelet spectra of buoyant atmospheric turbulence, in C. K. Chui, L. Montefusco, and L. Puccio, (eds.), *Wavelets: Theory, Algorithms, and Applications,* San Diego: Academic Press, 1994, pp. 533–541.

60. A. Druilhet et al., Experimental study of inhomogeneous turbulence in the lower troposphere by wavelet analysis, in C. K. Chui, L. Montefusco, and L. Puccio, (eds.), *Wavelets: Theory, Algorithms, and Applications,* San Diego: Academic Press, 1994, pp. 543–559.

61. M. V. Wickerhauser et al., Efficiency comparison of wavelet packet and adapted local cosine bases for compression of a two-dimensional turbulent flow, in C. K. Chui, L. Montefusco, and L.

Puccio, (eds.), *Wavelets: Theory, Algorithms, and Applications,* San Diego: Academic Press, 1994, pp. 509–531.

62. G. W. Wornell, *Signal Processing with Fractals: A Wavelet-Based Approach,* Upper Saddle River, NJ: Prentice Hall, 1966.
63. M. Hazewinkel, Wavelets understand fractals, in T. H. Koornwinder (ed.), *Wavelets: An Elementary Treatment of Theory and Applications,* River Edge, NJ: World Scientific, 1995, pp. 207–219.
64. M. Unser and A. Aldroubi, A review of wavelets in biomedical applications, *Proc. IEEE,* **84**: 626–638, 1996.
65. J. B. Weaver et al., Filtering noise from images with wavelet transforms, *Magn. Reson. Med.,* **24**: 288–295, 1991.
66. D. L. Donoho, De-noising by soft-thresholding, *IEEE Trans. Inf. Theory,* **41**: 613–627, 1995.
67. D. L. Donoho and I. M. Johnstone, Ideal spatial adaptation via wavelet shrinkage, *Biometrika,* **81**: 425–455, 1994.
68. R. A. DeVore and B. J. Lucier, Fast wavelet techniques for near-optimal image processing, *Proc. IEEE Military Commun. Conf.,* New York: IEEE, 1992, pp. 48.3.1–48.3.7.
69. J. Fan and A. Laine, Multiscale contrast enhancement and denoising in digital radiographs, in A. Aldroubi and M. Unser (eds.), *Wavelets in Medicine and Biology,* Boca Raton, FL: CRC Press, 1996, pp. 163–189.
70. W. Qian et al., Computer assisted diagnosis for digital mammography, *IEEE Eng. Med. Biol. Mag.,* **14**: 561–569, 1995.
71. W. Qian et al., Tree structured wavelet transform segmentation of microcalcifications in digital mammography, *Med. Phys.,* **22**: 1247–1254, 1995.
72. W. Qian and L. P. Clarke, Wavelet-based neural network with fuzzy-logic adaptivity for nuclear image restoration, *Proc. IEEE,* **84**: 1458–1473, 1996.
73. R. A. DeVore, B. Lucier, and Z. Yang, Feature extraction in digital mammography, in A. Aldroubi and M. Unser (eds.), *Wavelets in Medicine and Biology,* Boca Raton, FL: CRC Press, 1996, pp. 145–161.
74. J. J. Heine et al., Multiresolution statistical analysis of high-resolution digital mammograms, *IEEE Trans. Med. Imaging,* **16**: 503–515, 1997.
75. S. R. Deans, *The Radon Transform and Some of Its Applications,* New York: Wiley, 1983. Malabar, FL: Krieger, 1993.
76. F. Rashid-Farrokhi et al., Wavelet-based multiresolution local tomography, *IEEE Trans. Image Process.,* **6**: 1412–1430, 1997.
77. D. M. Healy, Jr. and J. B. Weaver, Adapted wavelet techniques for encoding magnetic resonance images, in A. Aldroubi and M. Unser (eds.), *Wavelets in Medicine and Biology,* Boca Raton, FL: CRC Press, 1996, pp. 297–352.

Reading List

In addition to Refs. 10, 23, 29, 34, 41, 46, 49, and 62 other possible texts are listed.

A. C. Cohen and R. D. Ryan, *Wavelets and Multiscale Signal Processing,* London: Chapman & Hall, 1995.

C. K. Chui, *An Introduction to Wavelets,* San Diego: Academic Press, 1992.

G. Kaiser, *A Friendly Guide to Wavelets,* Boston: Birkhäuser, 1994.

Y. Meyer, *Wavelets and Operators,* Cambridge: Cambridge University Press, 1992.

R. T. Ogden, *Essential Wavelets for Statistical Applications and Data Analysis,* Boston: Birkhäuser, 1997.

L. Prasad and S. S. Iyengar, *Wavelet Analysis with Applications to Image Processing,* Boca Raton, FL: CRC Press, 1997.

B. W. Suter, *Multirate and Wavelet Signal Processing,* Boca Raton, FL: Academic Press, 1998.

G. W. Walter, *Wavelets and Other Orthogonal Systems with Applications,* Boca Raton, FL: CRC Press, 1994.

P. Wojtaszczyk, *A Mathematical Introduction to Wavelets,* Cambridge: Cambridge University Press, 1997.

This list contains useful sources for applications. Most of these were not cited in the bibliography, but in a few cases there is overlap.

M. Akay (ed.), *Time Frequency and Wavelets in Biomedical Signal Processing,* New York: IEEE Press, 1998.

This is excellent for engineers and applied scientists. It covers time–frequency analysis methods with biomedical applications; wavelets, wavelet packets, and matching pursuits with biomedical applications; wavelets and medical imaging; and wavelets, neural networks, and fractals.

A. Aldroubi and M. Unser (eds.), *Wavelets in Medicine and Biology,* Boca Raton, FL: CRC Press, 1996.

This covers many applications in medicine and biology. The main topics are wavelet transform: theory and implementation, wavelets in medical imaging and tomography, wavelets and biomedical signal processing, wavelets and mathematical models in biology.

J. J. Benedetto and M. W. Frazier (eds.), *Wavelets: Mathematics and Applications,* Boca Raton, FL: CRC Press, 1994.

This is good for both foundations and applications. It contains core material, wavelets and signal processing, and wavelets and partial differential operators.

E. Foufoula-Georgiou and P. Kumar (eds.), *Wavelets in Geophysics,* San Diego: Academic Press, 1994.

A brief summary of wavelets is followed with applications directed toward turbulence and geophysics.

C. K. Chui (ed.), *Wavelets: A Tutorial in Theory and Applications,* San Diego: Academic Press, 1992.

This reference contains many articles on foundations for applications. There are sections on orthogonal wavelets, semi-orthogonal and nonorthogonal wavelets, wavelet-like local bases, multivariate scaling functions and wavelets, short-time Fourier and window-Radon transforms, theory of sampling and interpolation, and applications to numerical analysis and signal processing.

L. L. Schumaker and G. Webb (eds.), *Recent Advances in Wavelet Analysis,* San Diego: Academic Press, 1994.

The articles here are mainly on recent advances related to mathematical properties of wavelets.

C. K. Chui, L. Montefusco, and L. Puccio (eds.), *Wavelets: Theory, Algorithms, and Applications,* San Diego: Academic Press, 1994.

Several fundamentals are covered. These include multiresolution and multilevel analysis, wavelet transforms, spline wavelets, other mathematical tools for time–frequency analysis, wavelets and fractals, numerical methods and algorithms, and applications.

W. Dahmen, A. Kurdila, and P. Oswald (eds.), *Multiscale Wavelet Methods for Partial Differential Equations,* San Diego: Academic Press, 1997.

This will be of interest to people working with processes involving differential and integral equations, fast algorithms, software tools, numerical experiments, turbulence, and wavelet analysis of partial differential operators.

M. Farge, J. C. R. Hunt, and J. C. Vassilicos (eds.), *Wavelets, Fractals, and Fourier Transforms,* Oxford: Clarendon Press, 1993.

The papers here are based on the proceedings of a conference held at Newnham College, Cambridge in December 1990.

M. B. Ruskai et al. (eds.), *Wavelets and Their Applications,* Boston: Jones and Bartlett, 1992.

There are some very useful articles in this reference. It includes signal analysis, numerical analysis, wavelets and quantum mechanics, and theoretical developments.

J. M. Combes, A. Grossmann, and Ph. Tchmitchian (eds.), *Wavelets: Time–Frequency Methods and Phase Space,* 2nd ed., Berlin: Springer-Verlag, 1990.

The conference proceedings of a conference held at Marseille, France in 1988 are contained here. This brought together an interdisciplinary mix of participants, including many major contributors to the development of wavelet methods.

Y. Meyer (ed.), *Wavelets and Applications,* Berlin: Springer-Verlag, 1992.

The proceedings of an international conference on wavelets held at Marseille are in this volume. This conference along with the previous one illustrates and captures some of the flavor and excitement of time.

A. Antoniadis and G. Oppenheim (eds.), *Wavelets and Statistics,* Lecture Notes in Statistics 103, New York: Springer-Verlag, 1995.

This contains the proceedings of a conference on wavelets and statistics held at Villard de Lans, France in 1994.

T. H. Koornwinder (ed.), *Wavelets: An Elementary Treatment of Theory and Applications,* River Edge, NJ: World Scientific, 1993.

This series of articles provides a good introduction to wavelets. It is available in paperback and could serve as a text for a one-semester course.

Finally, there are a few important issues of journals that have been devoted entirely to wavelets, and applications. These include: *IEEE Trans. Inf. Theory,* **38**: March 1992, Part II of two parts; *IEEE Trans. Signal Process.,* **41**: December 1993; *Proc. IEEE,* **84**: April 1996; *Ann. Biomed. Eng.* **23** (5), 1995. A fairly new journal is *Applied and Computational Harmonic Analysis,* started in 1993; many articles in this journal are devoted to wavelets and applications.

Stanley R. Deans
John J. Heine
Deepak Gangadharan
Wei Qian
Maria Kallergi
Laurence P. Clarke
University of South Florida

WAVE SCATTERING, ELECTROMAGNETIC. See Electromagnetic subsurface remote sensing.
WEATHER. See Meteorological radar.
WEBCASTING. See Broadcasting via internet.
WEB COMPUTING. See Network computing.
WEBER FUNCTIONS. See Bessel functions.
WEB PROGRAMMING. See Java, javascript, hot java.
WEB SERVICES. See Internet companies.